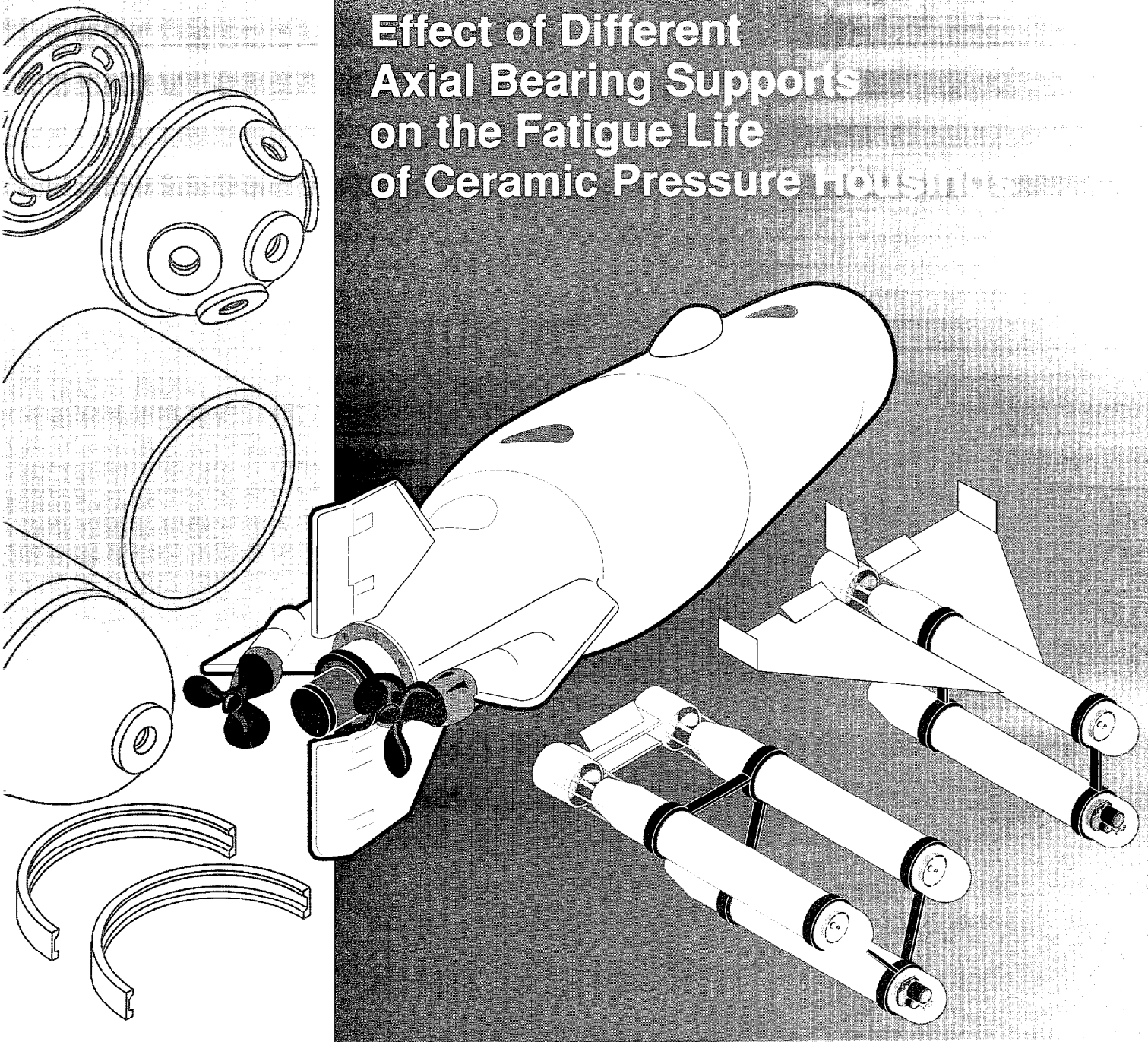


Effect of Different Axial Bearing Supports on the Fatigue Life of Ceramic Pressure Housings



R. P. Johnson
R. R. Kurkchubasche
J. D. Stachiw

Technical Report 1607
October 1993

Approved for public release; distribution is unlimited.



Technical Report 1607
October 1993

Effect of Different Axial Bearing Supports on the Fatigue Life of Ceramic Pressure Housings

R. P. Johnson
R. R. Kurkchubasche
J. D. Stachiw

**NAVAL COMMAND, CONTROL AND
OCEAN SURVEILLANCE CENTER
RDT&E DIVISION
San Diego, California 92152-5001**

K. E. EVANS, CAPT, USN
Commanding Officer

R. T. SHEARER
Executive Director

ADMINISTRATIVE INFORMATION

This work was performed by the Marine Materials Technical Staff, RDT&E Division of the Naval Command, Control and Ocean Surveillance Center, for the Naval Sea Systems Command, Washington, DC 20362.

SUMMARY

The fatigue life of underwater pressure housings composed of ceramic hull components assembled with epoxy-bonded metallic joint rings is dependent upon a number of parameters. The techniques used for bonding joint rings to the ceramic bearing surfaces is one such parameter that will affect the fatigue performance of pressure housings subjected to external pressure cycles. This report summarizes recent research aimed at identifying metallic joint-ring bonding methods that improve the cyclic life of ceramic pressure-housing assemblies. Several joining methods based on using an interlayer of various gasket materials as an axial bearing support between the ceramic hull and the metallic joint ring have been shown to improve the structural performance of ceramic pressure-housing assemblies. Three of the most promising meth-

ods identified are a thin intermediate layer of epoxy between the bearing surfaces of the joint ring and the ceramic hull, a graphite fiber-reinforced thermoplastic composite gasket bonded to the bearing surface of the ceramic hull, and a ceramic sacrificial ring bonded between the bearing surface of the metallic joint ring and the ceramic hull.

Based on these findings, four alumina-ceramic cylinders were assembled using various axial bearing support techniques, pressure cycled, and nondestructively evaluated to determine the extent of fatigue cracking that occurred during testing. While all four ceramic cylinders survived the external pressure cycling intact, the use of a thin layer of epoxy adjacent to the bearing surface of the ceramic cylinder was found to induce the least amount of fatigue damage in the ceramic hull bearing surface region.

CONTENTS

INTRODUCTION	1
BACKGROUND	2
TEST PLAN	4
TEST ASSEMBLIES	5
TEST CONFIGURATION A	5
TEST CONFIGURATION B	6
TEST CONFIGURATION C	6
TEST CONFIGURATION D	7
TEST RESULTS	7
FINDINGS	8
CONCLUSIONS	9
RECOMMENDATIONS	10
GLOSSARY	11
REFERENCES	12
 FIGURES	
1. Fatigue cracks in ceramic cylinders	13
2. Detail of ceramic cylinder with ceramic sacrificial ring axial bearing support	13
3. Test Configuration A	14
4. Test Configuration B	14
5. Test Configuration C	15
6. Test Configuration D	15
7. Test Configuration A cylindrical assembly components	16
8. 12.047-OD segmented construction ceramic cylinder	17
9. 12.047-OD axial bearing support study cylinder end cap	18
10. Axial bearing support study paper gasket, Sheet 1	19
10. Axial bearing support study paper gasket, Sheet 2	20
11. 11.890-OD segmented construction ceramic cylinder	21

FEATURED RESEARCH

12.	11.890-OD axial bearing support study cylinder end cap	22
13.	Axial bearing support study composite gasket	23
14.	Axial bearing support study continuous paper gasket	24
15.	Pressure-testing assembly	24
16.	Placement of Test Configuration D into pressure-testing vessel	25
17.	12-inch flat end plate	26
18.	12-inch cylinder Mod 1 end-cap O-ring	27
19.	Tie rod	28
20.	Flat end plate plug	29
21.	Bearing surface cracks at the top end of the Test Configuration B cylinder	30
22.	Crack-free bearing surface at the bottom end of the Test Configuration B cylinder	30
23.	Bearing surface cracks at the top end of the Test Configuration C cylinder	31
24.	Internal cracks detected ultrasonically at the top end of the Test Configuration A cylinder	31
25.	Internal cracks detected ultrasonically at the bottom end of the Test Configuration A cylinder	32
26.	Ultrasonic C-scans of Test Configuration A cylinder ends	32
27.	Ultrasonic C-scans of Test Configuration B cylinder ends	33
28.	Ultrasonic C-scans of Test Configuration C cylinder ends	33
29.	Ultrasonic C-scans of Test Configuration D cylinder ends	34
30.	Remains of Test Configuration A sacrificial ceramic ring after pressure testing	34
31.	Radial stress-contour plot of ceramic cylinder/ceramic sacrificial ring interface	35

TABLES

1.	Material properties of Coors Ceramic Company's alumina-ceramic compositions	37
2.	Material properties of the cured epoxy bonds between titanium joint rings and alumina-ceramic hulls	38
3.	Die-penetrant inspection findings of axial bearing surfaces	39
4.	Ultrasonic inspection findings of axial bearing surfaces	39

INTRODUCTION

The material properties of commercially available engineering ceramic compositions make them an attractive choice for designing external pressure housings for ocean engineering applications. Ceramics have superior properties of specific compressive strength, specific modulus, heat-transfer coefficients, and resistance to corrosion, as well as low material cost and a mature manufacturing base. External pressure housings constructed with ceramic hull components offer clear advantages over equivalent metallic housings when minimum dry weight and maximum operational buoyancy are desired.

Typical ceramic pressure housings consist of ceramic hemispherical and cylindrical components joined together with epoxy-bonded metallic joint rings. Joint rings used for ceramic housing assemblies generally have been machined from titanium alloy Ti-6Al-4V, although high-strength aluminum alloys have also been used. Metallic joint rings serve a variety of functions critical to the successful design of ceramic pressure housings (reference 6).

Metal joint rings act to transfer load between adjacent ceramic sections without having the bearing surface at the end of one ceramic part bear directly against the bearing surface of an adjacent ceramic part. Protecting the ends of ceramic components with metallic joint rings allows transfer of pressure-induced interface loads between hull sections while controlling fretting failure of ceramic bearing-surface ends.

Joint rings also provide local attachment points for mounting internal or external hardware such as tie rods, payload rails, and electrical cable raceways. The means for maintaining seals and closure between adjacent housing sections can be designed into the metallic joint rings. By integrating these features into the joint ring, the localized loads associated with handling, assembling, and sealing the pressure housing can be directed onto the metallic joint rings and not onto the more sensitive alumina hull components. The structural behavior of ceramic is such that it is well suited to

bearing the primarily compressive membrane stresses that exist in the shell walls of underwater pressure housings subject to depth loading. On the other hand, ceramic will not perform as well in areas where localized stresses exist. For this reason, metallic joint rings are an advantage in helping to buffer the ceramic hull sections against any extraneous stresses that may exist at joint interfaces.

Additionally, it may be advantageous to design metallic joint rings to provide additional stiffness to increase the buckling resistance of the ceramic pressure housing assembly. Metallic joint rings can be configured to provide the required ceramic-hull end support needed to achieve the operating depths for which the pressure housing is intended.

Although metallic joint rings provide functions that are essential to the practical design of ceramic housings, their presence can have a substantial impact on the structural performance of ceramic components when subjected to external pressure loading. Bearing surfaces at the ends of ceramic hull sections can undergo localized tension due to material and geometric discontinuities that exist at the interface between the ceramic hull and metallic joint rings when the housing assembly is under depth loading. Circumferential cracks have been observed to initiate from pre-existing flaws on the bearing surfaces of ceramic hull components where pressure-induced tensile stresses are calculated to exist. Over repeated pressure cycles, the sub-critical cracks can propagate meridionally into the ceramic shell wall as shown in figure 1¹ (reference 10). The structural integrity of the ceramic hull is compromised only when these cracks have propagated to the point that flakes of the ceramic wall spall off and failure occurs due to leakage and/or a reduction in the amount of material in the shell wall that can bear compressive load. Tensile stresses at levels well below the flexural strength of the ceramic composition are known to be sufficient to induce crack growth when present over a number of external pressure cycles.

1. Figures and tables are placed at the end of the text.

There are a number of approaches that can be used to curtail crack growth in axial bearing surface regions of ceramic hull components. The use of ceramic compositions that are less susceptible to crack growth (i.e., have increased toughness) is one avenue that could be pursued (references 7 through 9). Specification of the techniques used to finish grind the bearing surfaces of ceramic-hull component ends can affect cyclic life (reference 11). Another approach is to use intermediate materials between the ceramic hull and metallic joint ring that aid in protecting the ceramic bearing surface from crack initiation and propagation. A reduction in external pressure loading on the housing lowers the stress state in ceramic, which would also lead to increased cyclic life of the housing assembly. A final step is to perform detailed analysis and testing of the joint-ring design and assembly techniques to control the design variables that contribute to tensile stresses in the ceramic bearing-surface region.

There are a number of joint-ring design details that affect the level of tensile loading that occurs at the interface between the metallic joint rings and ceramic hull under external pressure loading. External pressure on underwater housings results in substantial compressive membrane strains in the hull sections. This meridional and circumferential compression leads to radial expansion of the housing wall under depth load. The amount of radial expansion depends on the elastic moduli and Poisson's ratio of the housing materials and the magnitude of the membrane stresses, referred to as the Poisson's effect. At discontinuities in the housing wall materials and geometry, like that at the interface between ceramic hull and metallic joint ring, a mismatch in radial expansion can occur. Typically, the metallic end cap will undergo greater radial expansion than the relatively stiff adjacent ceramic shell and place the ceramic bearing-surface region into localized tension.

Mismatches in radial deflection also can increase tensile loads on ceramic bearing surfaces at the joint ring interface. Unmatched deflections can be caused by differences in stiffness of adjacent sections under depth loads, or by thermal expansion differences of adjacent sections under temperature

loads. Unmatched deflections result in bending that increases the maximum bearing stresses at the ceramic ends, which increases the Poisson's effect. Similarly, surface irregularities can result in locally high bearing stresses in the ceramic at "high" spots on the ceramic component ends, leading to higher Poisson's-effect induced tensile loads.

A more subtle mechanism that can affect the level of tensile loads that exist in the bearing surface region and, consequently, affect the fatigue life of ceramic components, is the selection of bonding materials, bonding techniques, and assembly clearances used at the metallic joint ring/ceramic hull interface. These assembly details, which are the primary focus of this report, can have a substantial impact on the structural performance of ceramic pressure housings subjected to repeated external pressure cycles. The intent of this report is to summarize recent exploratory research that has been performed on axial bearing-surface supports used in the assembly of metallic joint rings to ceramic hulls for external pressure housings. Prior findings are reviewed, and the results of four cyclic pressure tests performed with alumina-ceramic pressure hulls assembled with titanium joint rings and various axial bearing-surface supports are presented.

BACKGROUND

Underwater pressure housings constructed with metallic joint rings and hulls fabricated from brittle materials such as ceramic have been known for years to be susceptible to failure by fracture of the hull sections when subjected to external pressure loading cycles. To prevent this type of failure, a substantial amount of effort has been devoted to developing joint-ring assembly techniques that improve the cyclic life of ceramic pressure housings. Much of the focus of this research has been on selecting materials that can be used as intermediate gaskets between titanium-alloy joint rings and the ceramic hull to improve the structural performance of the housing assembly for external pressure cycle loading (references 1 and 13). The scope of this research has run from screening tests performed with samples of gasket candidates compressively loaded between ceramic and

titanium anvils with a servo-hydraulic testing machine, up to full-scale pressure testing of cylindrical ceramic housings assembled with annular gaskets and joint rings.

The study of gasket materials that act as axial bearing-surface supports for ceramic component ends encapsulated with titanium joint rings has included testing of elastomeric materials, polymers, continuous fiber-reinforced polymer matrix composites, and high-strength metals. Criteria for axial bearing-surface support materials that extend the cyclic life of the ceramic housing assembly include the requirement that they have adequate strength to transfer load between the ceramic hull and titanium joint ring without exhibiting any type of material failure. Axial bearing-surface support materials with intermediate to high modulus and a similar Poisson's ratio to ceramic also would appear to be advantageous for reducing tensile stresses during depth loading caused by the Poisson's effect described earlier. Additionally, it would seem beneficial to use materials that are compliant enough to deform in the region of local surface irregularities on the ceramic ends.

Previous testing (references 1 and 13) of axial bearing-surface support materials indicates that elastomeric materials and high-strength metals are unacceptable as gasket candidates. In general, elastomeric materials were unable to withstand the high-compressive loading and tended to extrude from the ceramic/metal interface. Metal gaskets (lead, aluminum, copper, copper-beryllium alloy, hastalloy, inconel, and steel) with a range of values for elastic modulus and Poisson's ratio were found to lead to fracture of the adjacent ceramic bearing surface at a relatively low number of loading cycles. The best test results were obtained by using either fiber-reinforced polymer matrix composites as axial bearing-surface support gaskets or a thin interface layer of epoxy (references 1 and 13). A continuous high-modulus graphite fiber-reinforced poly-ether-ether-ketone (GFR PEEK) gasket gave the best performance while subjected to compressive loading cycles when compared to other composites such as continuous high-modulus graphite fiber-reinforced epoxy, glass fiber-reinforced epoxy, and extended polyethylene

fiber fabric (Spectra) reinforced epoxy. The use of a layer of epoxy to buffer the ceramic bearing-surface ends from the surface of the titanium joint ring also was found both experimentally and analytically to give adequate external pressure cycle life as long as the thickness of the epoxy was kept at approximately 0.010 of an inch or less (references 12 and 13).

The GFR PEEK composite gaskets tested were fabricated by laminating 8 plies of 0/90 graphite fiber tape with a PEEK matrix to form a 0.040-inch-thick sheet. It is hypothesized that the GFR PEEK gasket extends the cyclic life of ceramic test specimens because of its specially tailored mechanical properties. The GFR PEEK lamina has good in-plane stiffness so that it resists transverse deformations when sandwiched between compressively loaded ceramic and titanium test specimens. Low transverse strains lead to low transverse tensile stresses induced on the ceramic bearing surface. On the other hand, in directions perpendicular to the plane of the graphite fibers, i.e., normal to the gasket bearing surfaces, the gasket is relatively less stiff, owing to the flow properties of the PEEK matrix. Thus, the gasket is compliant around surface irregularities that exist on the ceramic bearing surface, which aids in reducing any locally high bearing stresses in the ceramic. The graphite fibers also have good lubrication properties which could aid in de-coupling the transverse displacements of the ceramic bearing surface from the transverse displacements of the gasket and the adjacent metallic joint ring bearing surface. Finally, the GFR PEEK gaskets have adequate strength and excellent tribological properties such that it can withstand the severe loading associated with repeated compression cycles.

A thin layer of epoxy was obtained by bonding the ceramic test specimens to the titanium test specimens using different types of spacers to control the thickness of the interface layer of epoxy. Good cyclic life was obtained by assembling ceramic pressure housings with a thin layer of epoxy at the axial bearing surfaces adjacent to the titanium joint rings as well as by assembling ceramic cylinders with sacrificial ceramic rings using interlayers of

epoxy as shown in figure 2 (reference 13). The use of a ceramic ring aids in isolating the region of the ceramic shell wall through which cracks propagate. Cracks that originate on the bearing surface between the ceramic ring and titanium joint ring are allowed to propagate through the ceramic ring, but are stalled at an epoxy interface between the ceramic ring and the remainder of the ceramic hull. Since the ceramic ring is entirely encapsulated by the joint ring, cracks are limited from propagating into any portion of the ceramic hull outside the joint ring flanges, which reduces the chance for spalling to occur. The use of an interface as crack stopper is a well documented approach to increasing crack resistance or toughness even when the structure is composed of brittle constituents such as ceramic and epoxy (reference 2).

TEST PLAN

In the process of designing two alumina-ceramic pressure housings with outer diameters of 26 inches and 33 inches for ocean depth service of 20,000 feet (references 3 through 5), several scale-model housings were assembled and tested to validate various design approaches (references 6 and 13). The alumina cylinders used in these model housings were manufactured by Coors Ceramics Company using their nominal 94-percent alumina composition AD-94. Mechanical and physical properties given by Coors for AD-94 and for its other alumina compositions are shown in table 1. The Naval Command, Control and Ocean Surveillance Center (NCCOSC) RDT&E Division (NRaD) was able to obtain four additional alumina cylinders from Coors from excess parts that remained after the scale-model housing cylinders had been delivered. Two of these cylinders had nominal dimensions of 11.890 inches for the outer diameter (OD) and 0.355 inch for the wall thickness. The other two cylinders had nominal dimensions of 12.047 inches for the OD and 0.434 inch for the wall thickness.

The four cylinders were used to investigate the effect on fatigue life of various axial bearing-surface supports used in assembling titanium end-cap joint rings to 94-percent alumina-ceramic cylinders

when subjected to external pressure cycles. Each end of the four ceramic test cylinders was assembled with a titanium joint ring using different techniques based on the most promising methods described above that had previously produced the best fatigue life results. One of the cylinder ends was assembled with a titanium end-cap joint ring and a GFR PEEK gasket. Three of the cylinder ends were assembled with titanium end-cap joint rings and a thin intermediate layer of epoxy using three different spacer techniques. The remaining four cylinder ends were assembled with sacrificial ceramic rings with various interface assembly techniques between the titanium end-cap joint ring and sacrificial ceramic ring and between the sacrificial ceramic ring and ceramic cylindrical hull.

In performing these tests to evaluate the eight different axial bearing-surface support configurations, it was understood that all test results would be based on a single sample for each assembly technique. Although it would be impossible to make firm conclusions based on such a limited testing program, it was hoped that test results coupled with prior research would indicate a trend toward the best assembly techniques that provide for maximum fatigue life of ceramic pressure housings. By testing the four ceramic cylinders of identical composition and manufacturing to the same stress level for an equal number of cycles while assembled with identical titanium joint rings and end closures, it was assumed that any differences in structural performance would be primarily attributable to the differences in axial bearing-surface supports.

The test plan for each of the four cylinders was to cycle each cylinder to the same stress level for a total of 500 cycles. The two 12.047-inch OD by 0.434-inch wall cylinders were pressurized to an external pressure of 10,000 psi during each cycle. The two 11.890-inch OD by 0.355-inch wall cylinders were pressurized to an external pressure of 8,100 psi during each cycle based on scaling down the test pressure used for the 12.047-inch OD cylinders by the ratio of the cross-sectional areas of two different-size cylinders. Scaling the peak test pressure in this way was done to keep the nominal membrane stresses of $-140,000$ psi for the hoop

direction and $-70,000$ psi for the axial direction constant for each cylinder tested. All pressure testing was performed in tap water at ambient room temperature. Each pressure cycle consisted of a pressurization from 50 psi to the peak pressures given above and a depressurization back to 50 psi. The peak pressure was maintained during each cycle for one minute. Pressurization and depressurization rates did not exceed 10,000 psi/minute during testing.

The number of cycles and the stress level chosen for the pressure testing was selected to ensure that each of the four cylinders would survive the pressure testing intact in order to evaluate the effectiveness of the various axial bearing-surface support methods. After completion of the cyclic testing, the titanium end-cap joint rings were removed from both ends of the four ceramic cylinders with heat and the clamping fixture described in reference 13. After cleaning the bearing surfaces at the cylinder ends, dye penetrant was used to visually detect the presence of cracks that formed on the bearing surface during pressure testing. Additionally, each cylinder end was inspected using ultrasonic nondestructive evaluation (NDE) techniques to determine the extent of cracking that occurred for each of the eight axial bearing-surface support configurations.

TEST ASSEMBLIES

Figures 3 through 6 show the four cylinder assemblies that were tested for this report with the different axial bearing-surface supports that were selected for evaluation. The four cylinder test assemblies were designated Test Configuration A, Test Configuration B, Test Configuration C, and Test Configuration D.

TEST CONFIGURATION A

The major components used as Test Configuration A are shown in figure 7. Test Configuration A used one of the 12.047-inch OD cylinders shown as -2 of drawing SK9402-101 (figure 8). The top bearing surface of A (as oriented in figure 3) was assembled with a titanium end-cap joint ring based

on a Naval Ocean Systems Center (NOSC)² Mod 1, type 2 design as shown in figure 9. Assembly of the end-cap joint ring was based on NRaD standard bonding procedures as outlined in appendix A of reference 6.

After thorough cleaning of the interior surfaces of the joint ring and the top end of the ceramic cylinder, a 0.12-inch-thick layer of degassed epoxy mixture selected by NOSC was poured into the interior of the joint ring. Material properties of the cured epoxy mixture are presented in table 2 (reference 14). Fifteen paper segment spacers, shown as -4 in drawing SK9402-127 (figure 10, sheet 2), were then pressed down with a clean tool through the epoxy mixture to the bearing surface of the joint ring. The 15 paper segment spacers were equally spaced in the joint ring, and additional epoxy mixture was poured into the joint ring to fill about half the depth of the joint ring. The ceramic cylinder was centered over the joint ring and lowered into the joint ring interior which was partially filled with the epoxy mixture. After the cylinder had settled into the joint ring and had come to rest on the paper segments, excess epoxy was cleaned up, and the joint ring was left to cure.

The 0.010-inch-thick paper spacers used as axial bearing-surface supports in assembling the joint ring serve to ensure that there will always be a minimum of 0.010 inch of axial clearance between the bearing surfaces of the ceramic cylinder and the metallic joint ring. This axial clearance compensates for any surface irregularities that may exist in the diamond-ground bearing surfaces of the ceramic cylinder or in the machined bearing surfaces of the joint ring. The actual final axial clearance obtained using 0.010-inch-thick spacers is approximately 0.020 of an inch thick because of epoxy boundary layers that exist after assembly on both sides of the paper spacers. The thickness of this boundary layer can vary, as it is dependent on a number of parameters such as epoxy viscosity, assembly clearances, use of settling weights during assembly, etc. Without some type of spacer, it

2. NOSC is now Naval Command, Control and Ocean Surveillance Center (NCCOSC) RDT&E Division (NRaD).

is more difficult to control the axial clearance, and the possibility exists that the ceramic and joint ring bearing surfaces could come into contact at "high" spots, which is an undesirable situation as explained previously.

The other end of the Test Configuration A cylinder (the bottom bearing surface shown in figure 3) was assembled with a sacrificial ceramic ring per -1 of drawing SK9402-101 (figure 8). The bonding of the sacrificial ceramic ring and cylinder into the end-cap joint ring proceeded as described above. Paper segment spacers per -4 of drawing SK9402-127 (figure 10, sheet 2) again were used to ensure a minimum of 0.010 inch of axial clearance between the joint ring and sacrificial ring and between the sacrificial ring and the cylindrical hull.

TEST CONFIGURATION B

Test Configuration B, shown in figure 4, was assembled using one of the 11.890-inch OD alumina-ceramic cylinders shown as -2 in drawing SK9402-126 (figure 11). End-cap joint rings per drawing SK9402-111 (figure 12) were machined to encapsulate the ends of the smaller-OD cylinders. Nominal radial clearance, flange length, flange thickness, and bearing thickness were held constant for the joint rings used with the two different-size cylinders that were available for testing in this study.

The top end of the Test Configuration B cylinder was first assembled with the GFR PEEK composite gasket shown in figure 13. The GFR PEEK gasket was placed on the alumina cylinder with a centering fixture, and the interface between the OD and inner diameter (ID) of the cylinder and the edges of the gasket were sealed with a five-minute epoxy mixture. Sealing the edges of the gasket was done to prevent intrusion of epoxy into the interface of the ceramic cylinder bearing surface and the composite gasket during the next step of assembly. After curing of the protective gasket seals, the cylinder was centered over the end-cap joint ring (partially filled with epoxy mixture) and was lowered. No additional spacers were used for axial clearance between the composite gasket and the bearing surface of the joint ring.

The bottom end of the Test Configuration B cylinder was assembled in a similar manner with an end-cap joint ring per drawing SK9402-111. For this end, no axial bearing-surface supports (i.e., no axial spacers) were used during the bonding of the end-cap joint ring. The end was centered over the joint ring and lowered into place, allowing the cylinder to settle into the epoxy mixture with its own weight. After the pressure testing of Test Configuration B cylinder was completed and the joint rings were removed for inspection of the ceramic bearing surfaces, the thickness of the straight epoxy interface layer at the bottom of the B assembly was measured to range from 0.008 to 0.010 of an inch thick.

TEST CONFIGURATION C

The second 12.047-inch OD cylinder used as Test Configuration C (figure 5) was assembled with sacrificial ceramic rings for axial bearing supports per -1 of drawing SK9402-101 (figure 8) at each end. At the top end of cylinder C, a dry 0.010-inch-thick paper gasket per -3 of drawing SK9402-127 (figure 10, sheet 2) was used as a spacer between the cylinder and the sacrificial ring. This was accomplished by centering the ring on the cylinder with the gasket between, and sealing, both the OD and ID of the interface with a five-minute epoxy mixture. After the interface seal cured, the end-cap joint ring was bonded into place with a 0.010-inch-thick paper gasket per -2 of drawing SK9402-127 (figure 10, sheet 1) as an axial-spacer/bearing-surface support between the sacrificial ring and the bearing surface of the joint ring. A photograph of the -2 paper gasket is shown in figure 14. This gasket provides the same axial clearance as the paper segments used with Test Configuration A, but because it is a continuous gasket, it is easier to assemble. Holes in the gasket allow epoxy to flow easily through when submerging it into the epoxy mixture to the joint ring bearing surface.

The bottom end of Test Configuration C cylinder also was assembled with a sacrificial ring, but no axial bearing-surface supports were used in the interface between the sacrificial ring and the cylinder. Instead, the sacrificial ring was bonded to the end of the cylinder with epoxy only and the aid of

a centering fixture. Again, the straight epoxy-cylinder/sacrificial-ring bond was measured to be approximately 0.010 of an inch thick after it had cured. An end-cap joint ring was then bonded into place, encapsulating the sacrificial ring/cylinder end, using a -2 paper gasket as a spacer between the sacrificial ring and the bearing surface of the titanium joint ring.

TEST CONFIGURATION D

The remaining 11.890-inch OD cylinder used as Test Configuration D had a sacrificial ring bonded to its top end as shown in figure 6. The finished top-end assembly had axial clearance maintained between the cylinder and the sacrificial ring (and the sacrificial ring and the end-cap joint ring) with the 0.010-inch-thick -1 paper gaskets per drawing SK9402-127 (figure 10, sheet 1) assembled with epoxy. The bottom end of the D cylinder was assembled with an epoxy-bonded joint ring, again using a -1 paper gasket as an axial-clearance spacer/bearing-surface support.

Each of the four test configurations were pressure tested using test hardware shown in figure 15. Figure 16 shows the test hardware again, with the Test Configuration D cylinder assembly being lowered into the pressure vessel for cyclic loading. Flat steel plates shown in figure 17 were used as end closures for all pressure testing. These massive end plates are not an ideal end closure design for ceramic housings where maximum fatigue life is desired. Rather, the end plates were designed to be robust enough to withstand extensive pressure testing and to survive catastrophic implosion of a cylinder assembly if that should occur. The O-ring shown in figure 18 was used to seal the interface between each end-cap joint ring and the flat end-plate closures. Closure was maintained with the four external-tensioned tie rods shown in figure 19. The plug shown in figure 20 was used with the flat end-plate closure that had a centerline through-hole which could be used to check for any leaks that might occur during testing.

TEST RESULTS

All four test configurations withstood the 500 external pressure cycles intact. Upon completion of testing, each cylinder assembly was shipped back to NRD where all titanium end-cap joint rings were removed in order to inspect the axial bearing-surface regions of each cylinder. After removal of each joint ring, the bearing surfaces were cleaned and dye penetrant was applied to detect the presence of any bearing-surface cracks that formed during pressure testing. Table 3 summarizes the results of the visual inspection of the four cylinder assemblies: Test Configurations A, B, C, and D.

The use of dye penetrant to determine the extent of bearing-surface cracks was fairly successful as confirmed subsequently through ultrasonic inspection. Much of the ability to detect cracks visually depended on how clean the bearing surfaces could be made before the application of dye penetrant. In some instances, fine short-circumferential-length cracks, that were detected ultrasonically, were not seen in the dye penetrant inspection. An example of the visual findings for Test Configuration B cylinder is shown in figures 21 and 22. Figure 21 shows the branched circumferential cracks that were found in the top axial bearing surface of the alumina cylinder adjacent to the GFR PEEK gasket. Figure 22 shows the other (bottom) end of the Test Configuration B cylinder where an approximately 0.010-inch-thick uniform epoxy layer (without spacers) was used to separate the bearing surface of the alumina cylinder from the bearing surface of the titanium joint ring. The bearing surface at the bottom end of B cylinder was essentially free of cracks with the exception of several very faint cracks detected in one locale.

In general, most circumferential cracks that were detected with dye penetrant were located at the mid-plane of the bearing surface. The two primary exceptions to this pattern were the cracks detected at the top end of Test Configuration B where the GFR PEEK gasket was used, and at the top end of Test Configuration C where the dry-paper gasket was used between the sacrificial ceramic ring and the ceramic cylinder. As seen in figure 21, the

cracks that formed with the GFR PEEK gasket tended to wander between mid-plane of the bearing surface and the OD of the bearing surface. Figure 23 shows the extensive cracking detected at the top end of Test Configuration C where numerous short-circumferential cracks ran parallel to one another throughout the bearing-surface thickness. In both of these cases, the bearing surface of the cylinder was free of epoxy.

Ultrasonic inspection of each of the four configurations was performed using a pulse-echo transducer. Each cylinder was fully submerged in an inspection tank and centered on a turntable. Equipment settings were calibrated using 94-percent alumina-ceramic witness specimens, and the C-scans were performed using a 0.050-inch index. Ultrasonic NDE C-scans generated for each test configuration cylinder show the extent to which the cracks have propagated axially into the shell wall from the bearing surface. Figures 24 and 25, derived from C-scans, show the internal cracks that formed in the cylinder of Test Configuration A. Figure 24 indicates that a maximum crack length of 5.5 inches existed after 500 cycles for the top end of Test Configuration A, where an axial support of epoxy and segmented paper spacers was used. Figure 25 shows the ultrasonic findings at the bottom end of Test Configuration A, where a maximum crack length of 1 inch was found where segmented paper spacers with epoxy were used between the cylinder and a sacrificial ceramic ring. C-scans cannot be used to determine whether multiple parallel circumferential cracks exist through the wall thickness as are present, for example, at the top end of Test Configuration C, shown in figure 23. However, ultrasonically generated A-scans may, in some cases, be used to determine if multiple parallel cracks exist during inspection.

Figures 26 through 29 show C-scans that were generated for each of the four test configurations with a summary of the findings given in table 4. Each C-scan strip represents a one-to-one scale, two-dimensional projection of the end of each cylinder. The length of each strip represents the circumference of the cylinder, and the width of each strip represents the axial length from the end of

each cylinder, which was scanned ultrasonically (i.e., each scan is a two-dimensional map of the cylinder volume adjacent to the bearing surface). The axial length of cylinder scanned for each cylinder end was determined by the extent to which the cracks had propagated from the bearing surface.

FINDINGS

The fact that all four cylinders survived the 500 cycles to the high stress levels selected with an array of different axial bearing-surface supports demonstrates the credible application of ceramic materials for external pressure housings. Approximate nominal membrane stress levels of $-140,000$ psi for hoop stress and $-70,000$ psi for axial stress were calculated to exist in the cylinders away from the joint regions at the peak pressure during each cycle. Even the Test Configuration A cylinder which was found to have cracks extending as long as 5.5 inches from the bearing surface survived 500 cycles without failure. Obviously, such long crack lengths are undesirable for reliable structural performance since once the crack length extends beyond the bond length of the end-cap joint ring (1.31 inches in this case), the chance for spalling of the cylinder wall would exist with its potentially degrading effects.

Study of the ultrasonic C-scans generated for this report would seem to indicate that the use of sacrificial ceramic rings with paper segments or paper gaskets does not appear to be a worthy means of extending the cyclic fatigue life of ceramic pressure housings. Results of Test Configuration A indicate that when substantial circumferential cracking initiates from the interface between the metallic joint ring and the sacrificial ceramic ring, the interface between the sacrificial ceramic ring and the ceramic cylinder does aid, somewhat, in impeding the cracks from propagating into the cylinder. Figure 30 shows the sacrificial ring used in Test Configuration A after it was removed from the joint ring after testing. The sacrificial ring was so riddled with circumferential cracks that it broke into the annular shards shown. Inspection of the cylinder bearing surface adjacent to the sacrificial ring did not show the level of cracking that existed in the sacrificial ring.

Meanwhile, inspection of ultrasonic findings for Test Configuration D indicates relatively little difference between the ends of the cylinder, even though one was protected by a sacrificial ring and one was not. In fact, the shallow depth of cracks detected at both ends would imply that the cracks that formed at the end protected with a sacrificial ring probably initiated from the epoxy boundary with a paper gasket between the sacrificial ring and the cylinder. If the epoxy/paper gasket interface layer between the sacrificial ring and cylinder initiates cracks, this would defeat the purpose of adding a sacrificial ring. Figure 31 shows a radial stress-contour plot from a finite-element analysis of the sacrificial-ring/cylinder-joint region under an external pressure of 10,000 psi. The epoxy layers are shown in red, the titanium joint ring is shown in purple, and the flat-end closure is shown in royal blue. The stress contours in the ceramic cylinder and ceramic ring predicts that the highest tensile stresses are occurring at the sacrificial-ring/cylinder interface instead of the joint-ring/sacrificial-ring interface. This is due, in part, to the unfortunate proximity of the termination of the end-closure lap joint with the sacrificial-ring/cylinder interface, but, none the less, indicates that the use of sacrificial rings is not necessarily a step forward for extending fatigue life of ceramic housings. In addition, sacrificial rings add more cost and increase the difficulty of assembling ceramic pressure housings. Only when the sacrificial ring was separated from the ceramic cylinder with a 0.010-inch-thick layer of neat epoxy, did no cracks initiate from the bearing surface at the cylinder end (bottom end of Test Configuration C).

GFR PEEK gaskets are also a relatively expensive means of providing axial support at the bearing surface of ceramic component ends in terms of cost and difficulty of assembly. The most attractive means of assembling metallic joint rings to ceramic ends as identified from the limited testing performed for this report, is a thin layer (0.010 of an inch, or less) of epoxy between the bearing surfaces of the cylinder end and the metallic joint ring. The least amount of sub-critical crack growth in the cylinder ends occurred in Test Configurations B and C where a uniform thin layer of epoxy without

spacers was used. As mentioned previously, the drawback of a straight epoxy layer without spacers is the increased complexity of assembling the housing while maintaining control of the axial clearance between the cylinder and joint ring. For this reason, axial spacers are still an attractive method for ensuring that a minimum clearance will always exist.

Of the two types of 0.010-inch-thick paper spacers tested for this report, the use of a continuous annular gasket (SK9402-127-1 or -2 of figure 10, sheet 1) gave a much better performance than the segmented spacers (SK9402-127-4 of figure 10, sheet 2). Not only did substantially less crack growth occur with the continuous gasket than with the segments, but the continuous gasket is easier to assemble. It is hypothesized that by using paper segments, the cylinder is essentially resting on an elastic foundation that is varying in stiffness because of the changes in properties of the paper segment/epoxy sectors and the straight epoxy gaps between the paper segments. This variation in stiffness induces bending of the ceramic end surface and, consequently, increases the maximum bearing surface stresses, which leads to increased local tensile stresses and the subsequent greater potential for crack growth.

CONCLUSIONS

Based on the limited scope of testing performed for this report, the following axial bearing-surface support methods are ranked in terms of their benefit for extending the cyclic fatigue life of alumina-ceramic cylinders:

1. The **best** axial bearing-surface support is provided by a sacrificial ceramic ring of the same composition as the cylindrical hull with 0.010-inch-thick straight epoxy layer at the joint-ring/sacrificial-ring and the sacrificial-ring/cylinder interface. If sacrificial ceramic rings are employed, the flange lengths of the end-cap joint ring should be increased to ensure that an axial bond length is maintained between the cylindrical hull and joint ring equal to at least twice the thickness of the cylinder.

2. The **second best** axial bearing-surface support is provided by a thin layer of straight epoxy between the bearing surfaces of the joint ring and the end of the ceramic cylinder.
3. The **third best** axial bearing-surface support is provided by a thin layer of epoxy with a continuous 0.010-inch-thick annular paper gasket between the bearing surfaces of the joint ring and the end of the ceramic cylinder. Even though an annular paper gasket coated with epoxy is not the best assembly technique (from a structural performance point of view), it is certainly the most economical approach in terms of hardware cost (no sacrificial ceramic rings, no GFR PEEK gaskets) and ease of assembly.
4. The **least** effective axial bearing-surface support technique is the use of a thin layer of epoxy with 0.010-inch-thick paper segments.

RECOMMENDATIONS

Based on these results, it appears that the best technique for assembling metallic joint rings to ceramic component ends for both maximum cyclic life and ease of assembly is a thin layer of epoxy at the axial bearing surface by itself or with the aid of a continuous 0.010-inch-thick annular paper gasket. It is recommended that further axial bearing-surface support research for assembling ceramic external pressure housings focus on the actual thickness of the epoxy layer that provides the best structural performance test results. Once the optimum axial clearance has been determined, a means of repeatedly achieving the desired clearance during assembly should be developed with the aid of new fixturing methods or through the use of paper spacers, or other types of spacers made from epoxy or similar materials.

GLOSSARY

GFR graphite fiber-reinforced

ID inner diameter

NDE nondestructive evaluation

NOSC Naval Ocean Systems Center

OD outer diameter

PEEK poly-ether-ether-ketone

REFERENCES

1. Burke, M. A. 1991. "The Selection and Testing of a Gasket Material to Interface Between Ceramic and Metallic Pressure Vessel Components," Westinghouse Science and Technology Center Document No. 91-8TC3-Gordn-R1 (Aug).
2. Gordon, J. E. 1968. "The New Science of Strong Materials," Princeton University Press, Princeton, New Jersey.
3. Johnson, R. P., R. R. Kurkchubasche, and J. D. Stachiw. 1993. "Design and Structural Analysis of Alumina Ceramic Housings For Deep Submergence Service: Fifth Generation Housings," NRaD TR 1583 (Mar). NCCOSC RDT&E Division, San Diego, CA.
4. Johnson, R. P., R. R. Kurkchubasche, and J. D. Stachiw. 1993. "Evaluation of Alumina Ceramic Housings for Deep Submergence Service: Fifth Generation Housings—Part I," NRaD TR 1584 (Jun). NCCOSC RDT&E Division, San Diego, CA.
5. Johnson, R. P., R. R. Kurkchubasche. 1994. "Evaluation of Alumina Ceramic Housings for Deep Submergence Service: Fifth Generation Housings—Part II," NRaD TR 1585. NCCOSC RD&TE Division, San Diego, CA.
6. Johnson, R. P., R. R. Kurkchubasche, and J. D. Stachiw. 1993. "Exploratory Study of Joint Rings for Ceramic Underwater Pressure Housings," NRaD TR 1586 (May). NCCOSC RDT&E Division, San Diego, CA.
7. Johnson, R. P., R. R. Kurkchubasche, and J. D. Stachiw. 1993. "Structural Performance of Cylindrical Pressure Housings of Different Ceramic Components Under External Pressure Loading Part II Zirconia Toughened Alumina Ceramic," NRaD TR 1593 (Jun). NCCOSC RDT&E Division, San Diego, CA.
8. Kurkchubasche, R. R., R. P. Johnson. 1993. "Structural Performance of Cylindrical Pressure Housings of Different Ceramic Compositions Under External Pressure Loading Part III Sintered Reaction Bonded Silicon Nitride Ceramic," NRaD TR 1592 (Jul). NCCOSC RDT&E Division, San Diego, CA.
9. Kurkchubasche, R. R., R. P. Johnson. 1993. "Structural Performance of Cylindrical Pressure Housings of Different Ceramic Compositions Under External Pressure Loading Part IV Silicon Carbide Particulate Reinforced Alumina Ceramic," NRaD TR 1594 (Aug). NCCOSC RDT&E Division, San Diego, CA.
10. Kurkchubasche, R. R., R. P. Johnson, and J. D. Stachiw. 1993. "Evaluation of Nondestructive Inspection Techniques for Quality Control of Alumina Ceramic Housing Components," NRaD TR 1588 (May). NCCOSC RDT&E Division, San Diego, CA.
11. Cox, B. L., M. K. Ferber, C. R. Hubbard, A. E. Pasto, M. L. Santella, W. A. Simpson, Jr., and T. R. Watkins. 1993. "Effect of Surface Condition on Strength and Fatigue Behavior of Alumina Ceramic," work performed by ORNL, Oak Ridge, TN, under MIPR No. N66001-92NP00120, NRaD TD 2584 (Oct). NCCOSC RDT&E Division, San Diego, CA.
12. Shields, W. 1992. "Ceramic/Metal Joint Design Report," Westinghouse Electric Corporation, Oceanic Division, Ocean Engineering Report 92-10 (Jul).
13. Stachiw, J. D., R. P. Johnson, and R. R. Kurkchubasche. 1993. "Evaluation of Scale-Model Ceramic Housings for Deep Submergence Service: Fifth Generation Housings," NRaD TR 1582 (Mar). NCCOSC RDT&E Division, San Diego, CA.
14. Correspondence between NRaD's Marine Materials Technical Staff and W. H. Gordon of Westinghouse Electric Corporation Oceanic Division, Annapolis, MD.

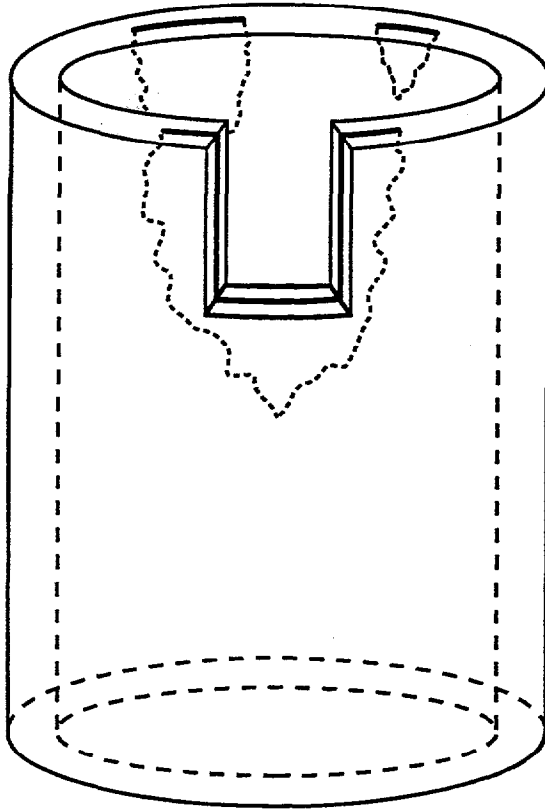


Figure 1. Fatigue cracks in ceramic cylinders.

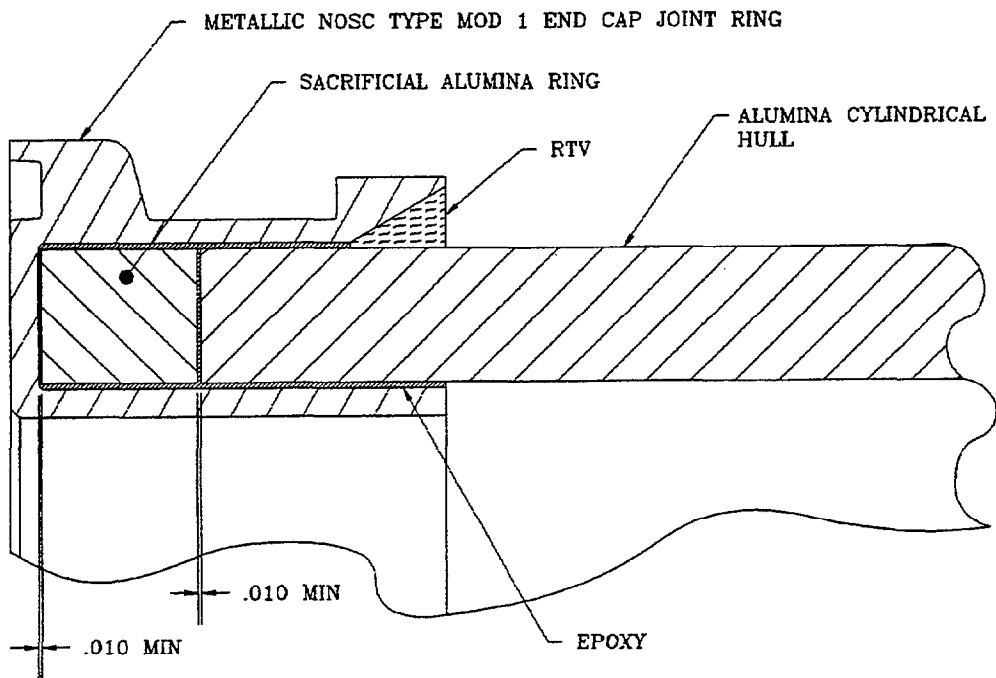


Figure 2. Detail of ceramic cylinder with ceramic sacrificial ring axial bearing support.

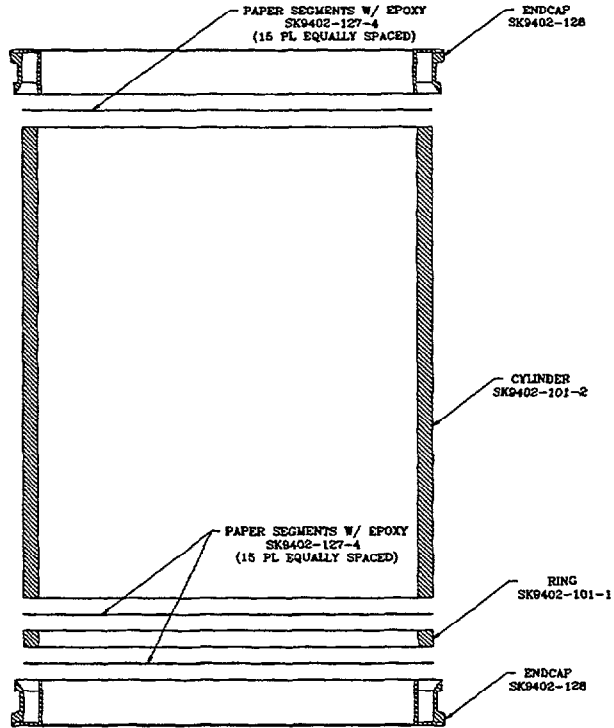


Figure 3. Test Configuration A.

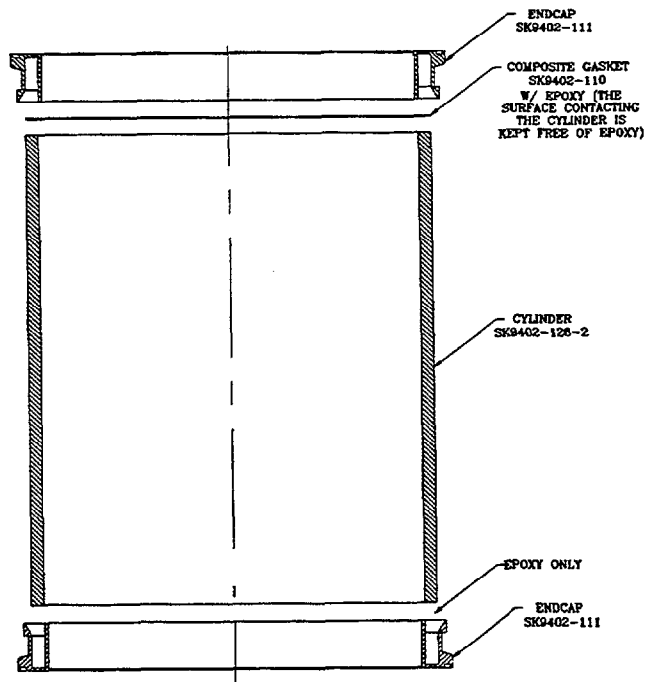


Figure 4. Test Configuration B.

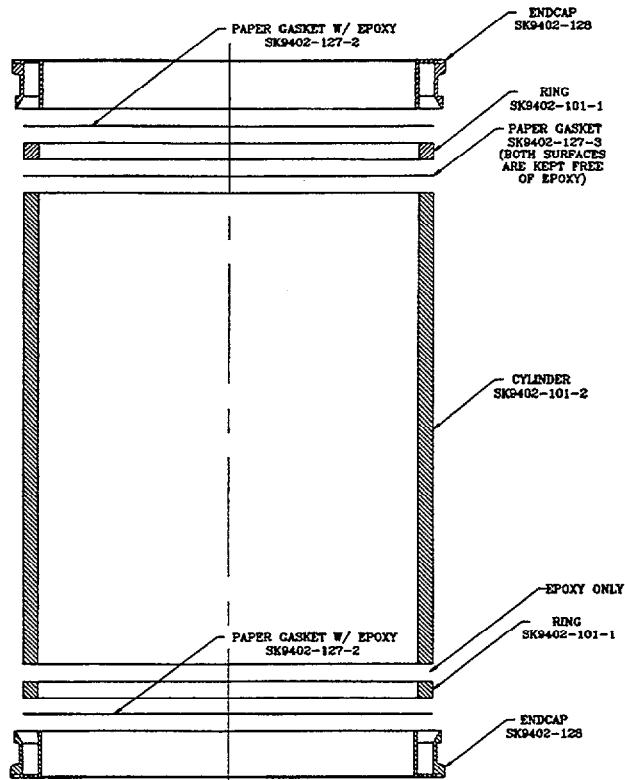


Figure 5. Test Configuration C.

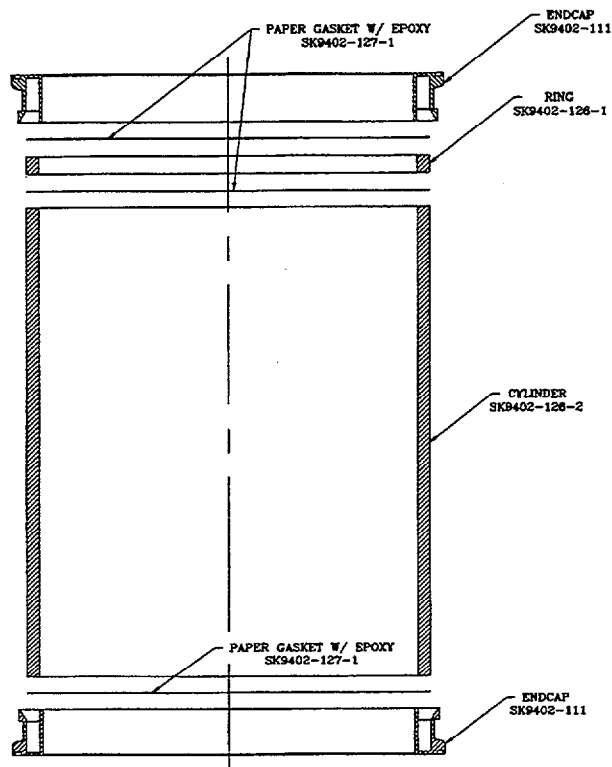


Figure 6. Test Configuration D.

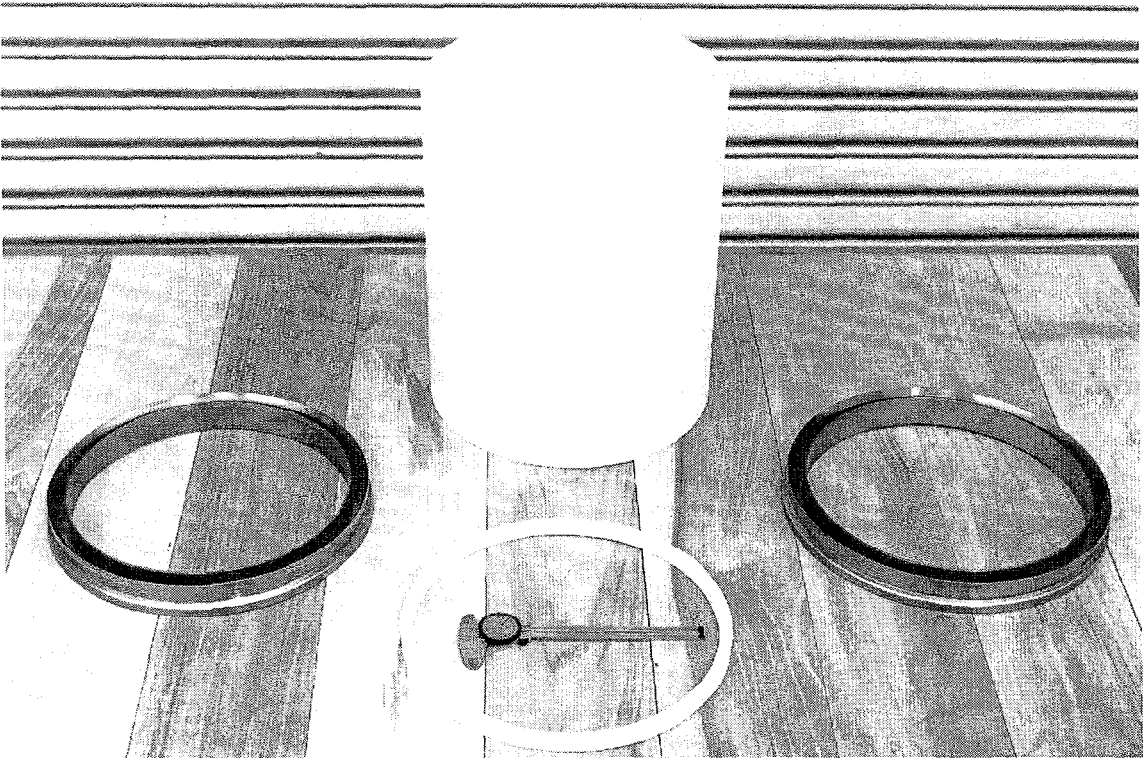


Figure 7. Test configuration A cylindrical assembly components.

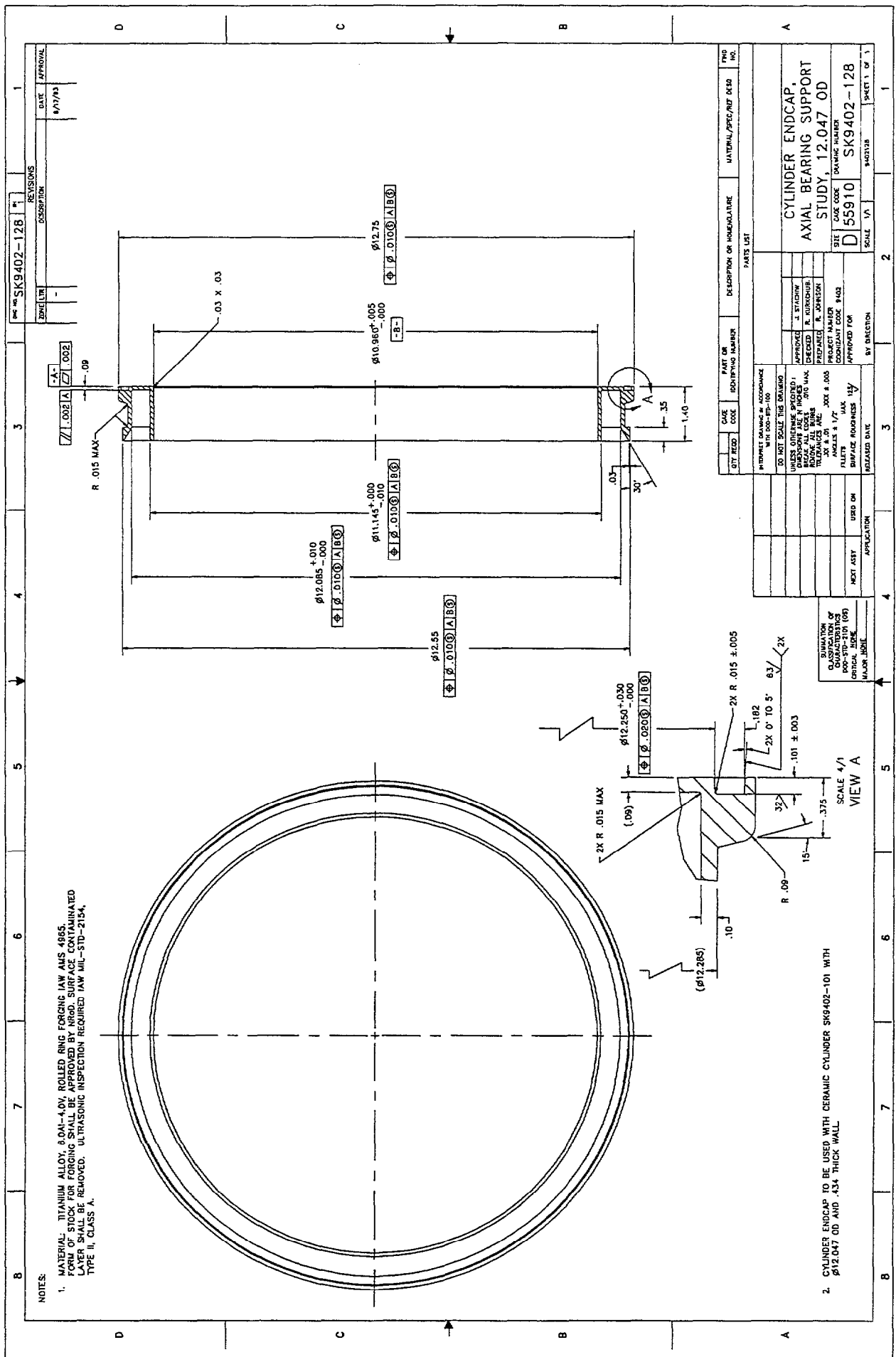


Figure 9. 12.047-OD axial bearing support study cylinder end cap.

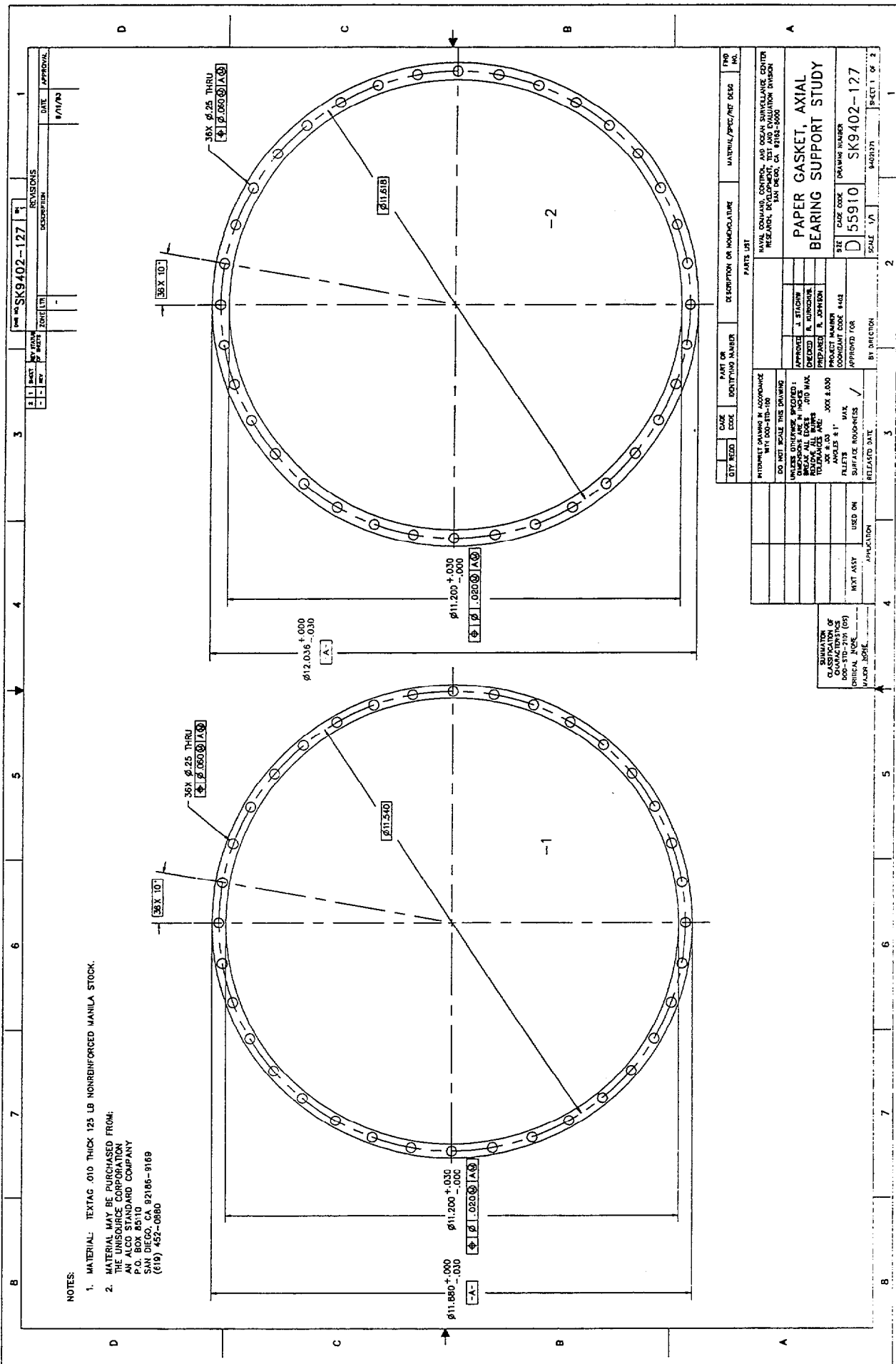


Figure 10. Axial bearing support study paper gasket, Sheet 1.

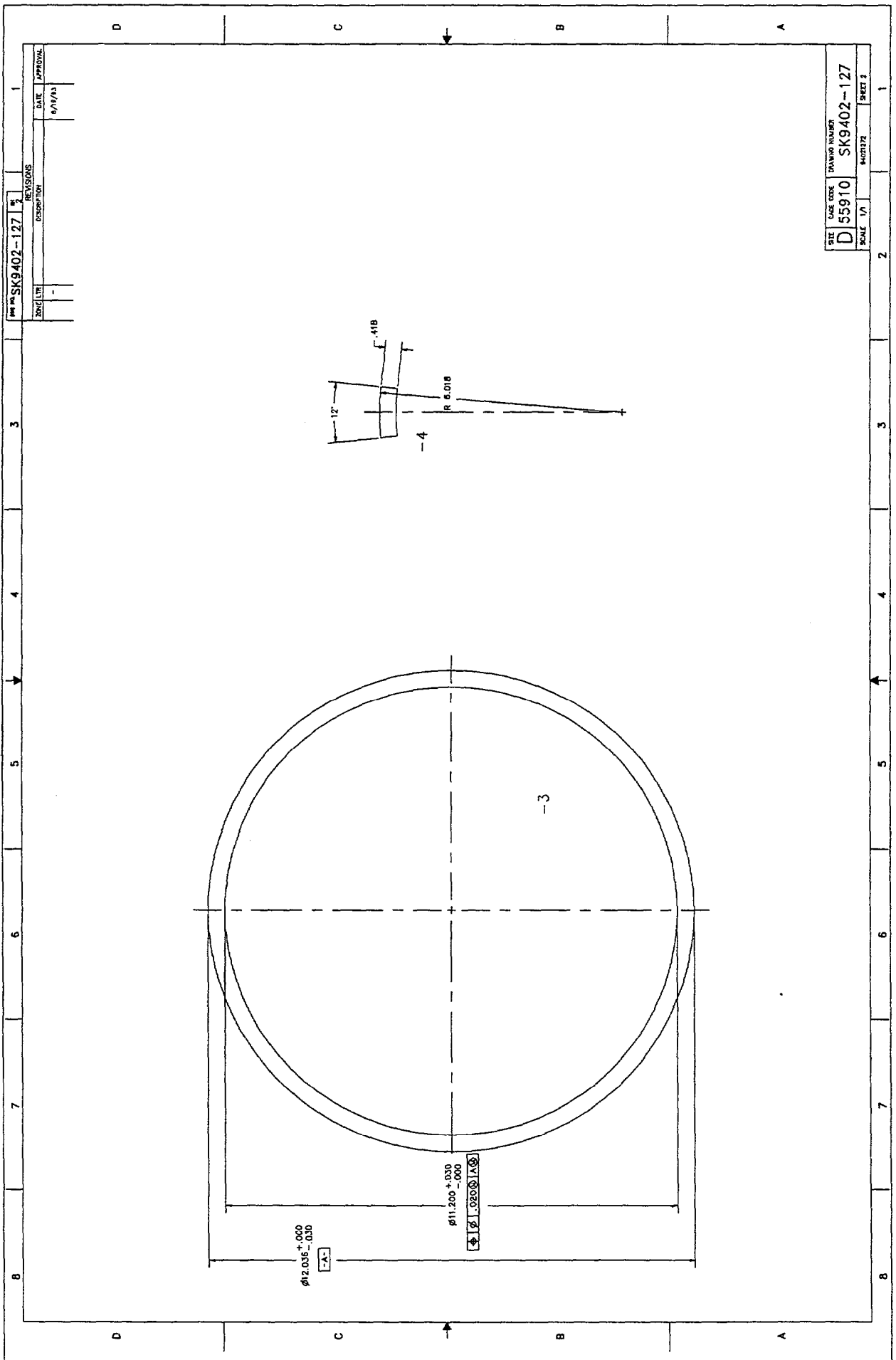


Figure 10. Axial bearing support study paper gasket, Sheet 2.

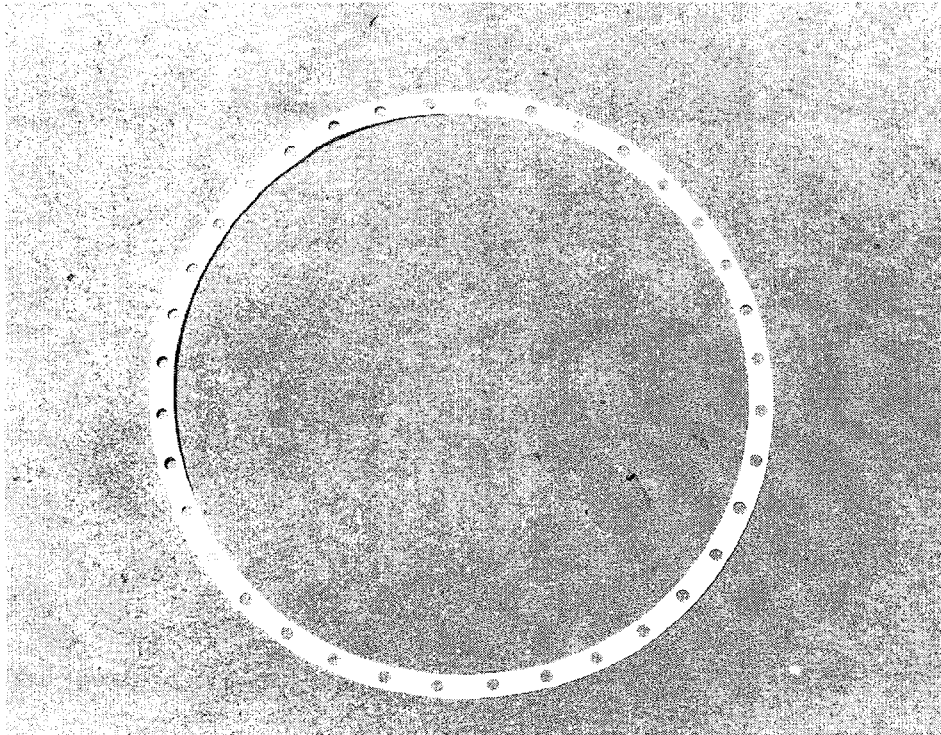


Figure 14. Axial bearing support study continuous paper gasket.

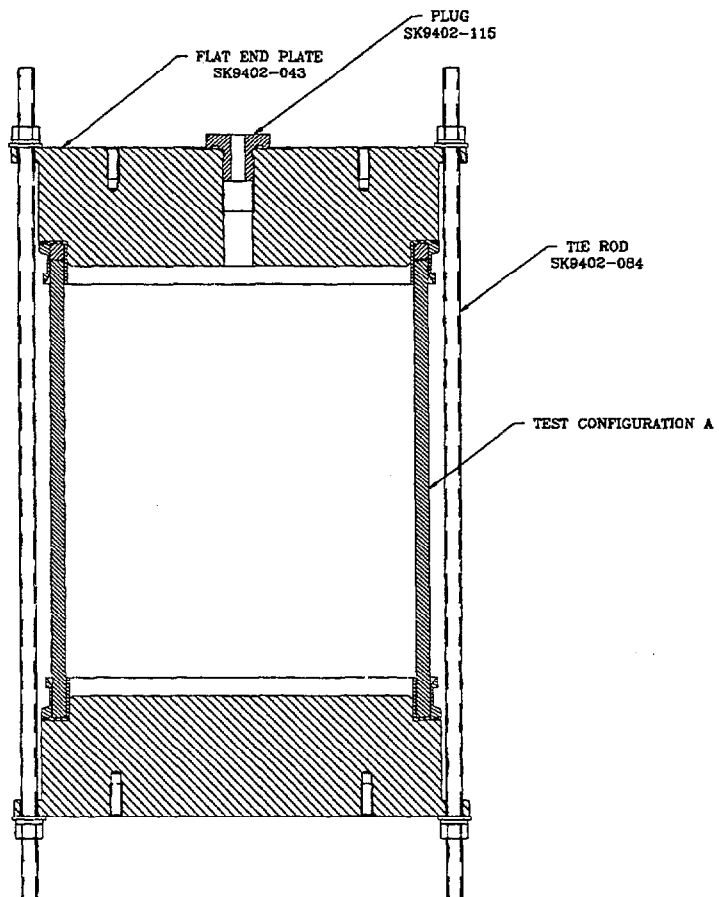


Figure 15. Pressure-testing assembly.

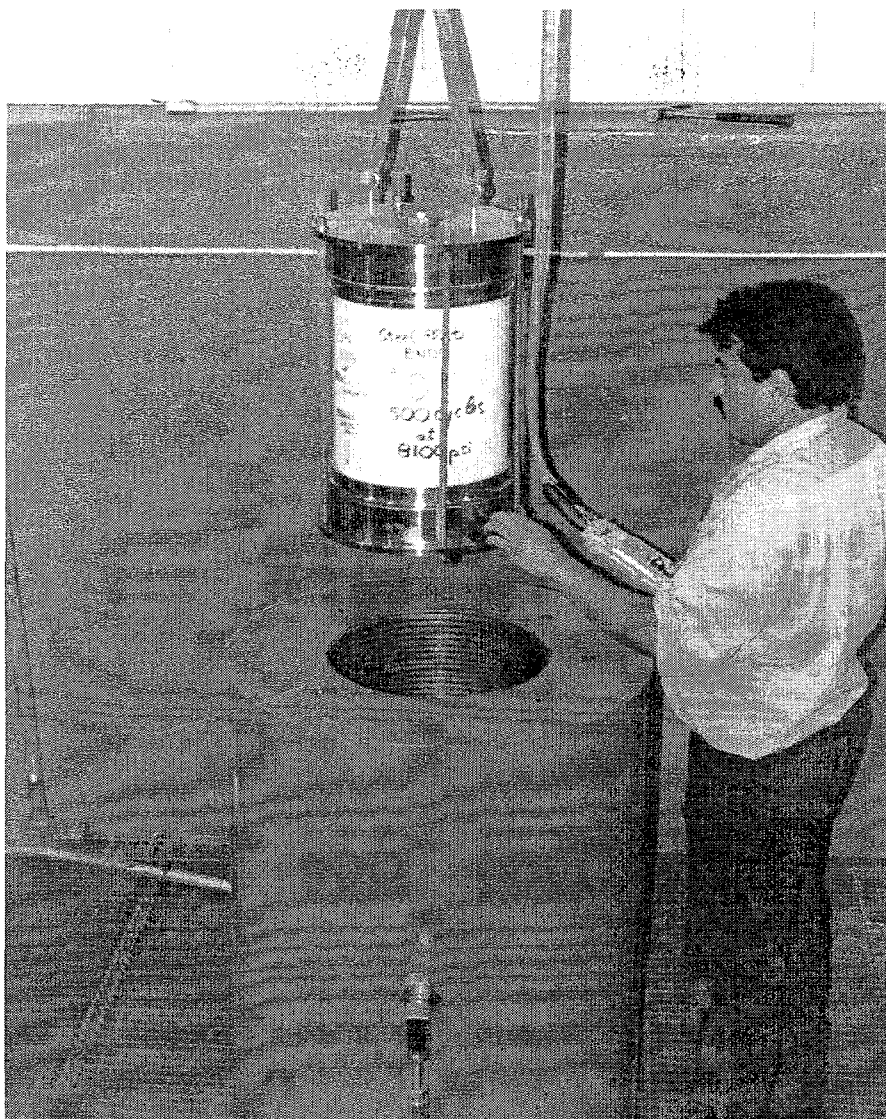


Figure 16. Placement of Test Configuration D into pressure-testing vessel.

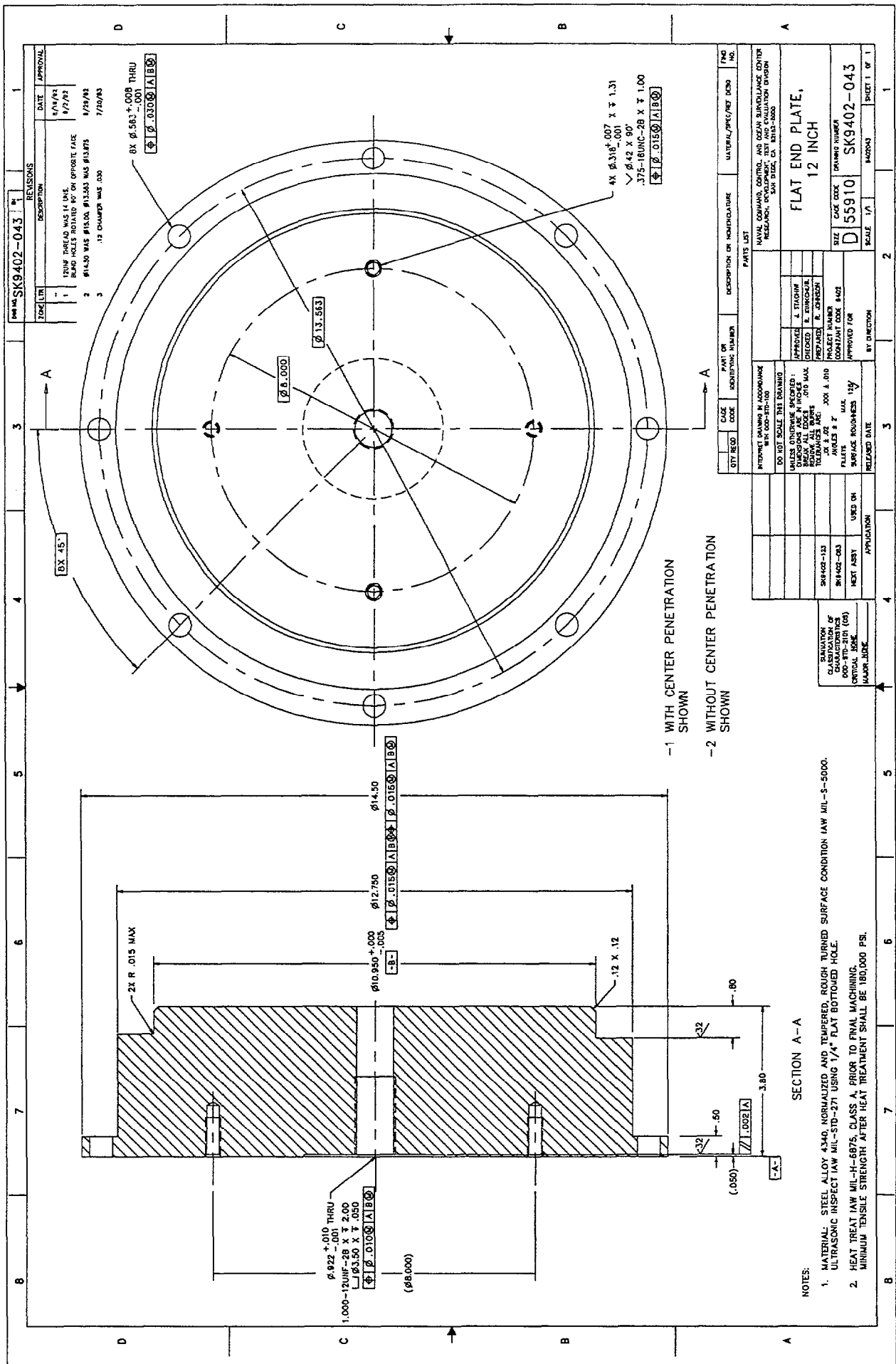


Figure 17. 12-inch flat end plate.

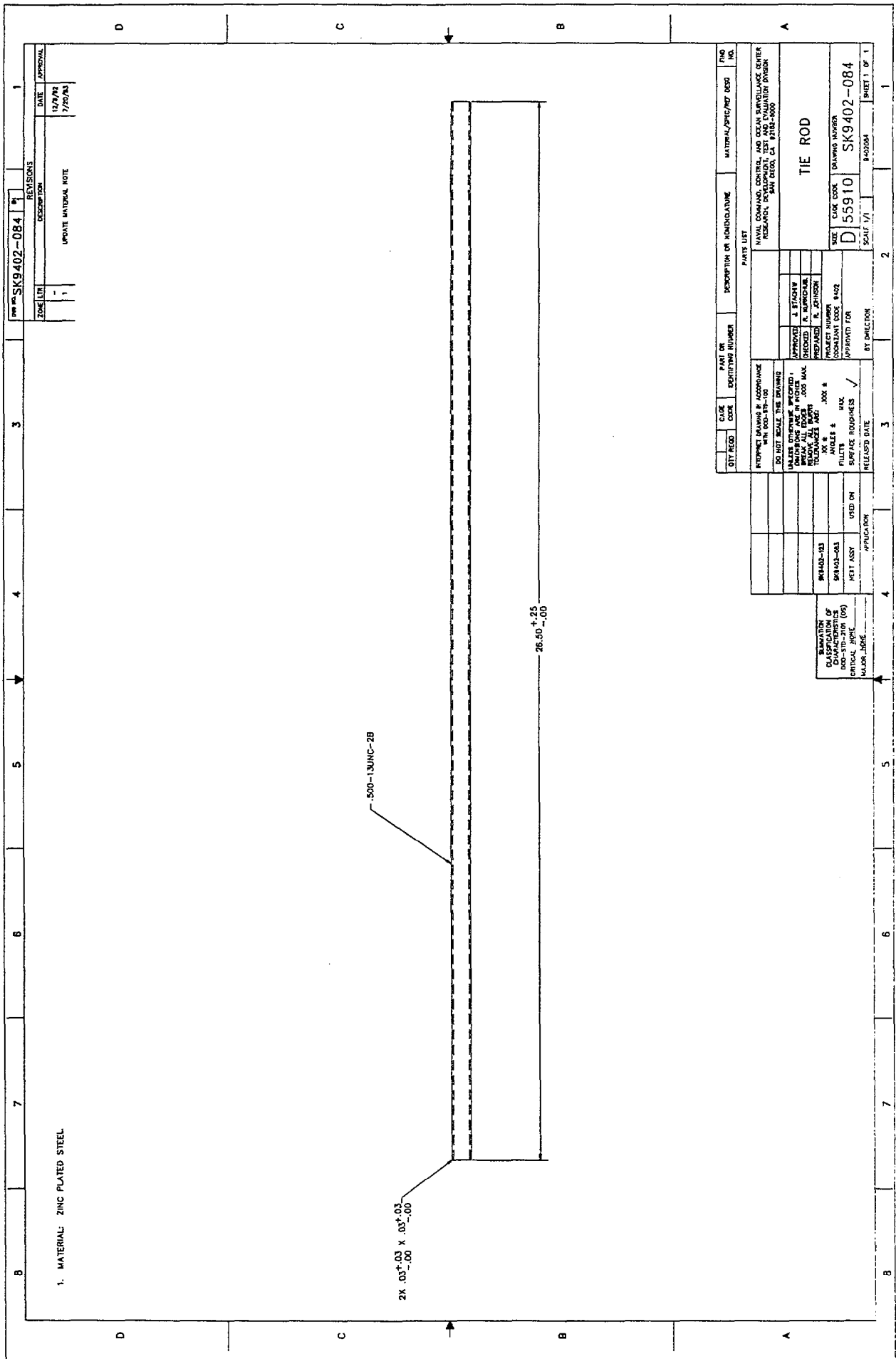


Figure 19. Tie rod.

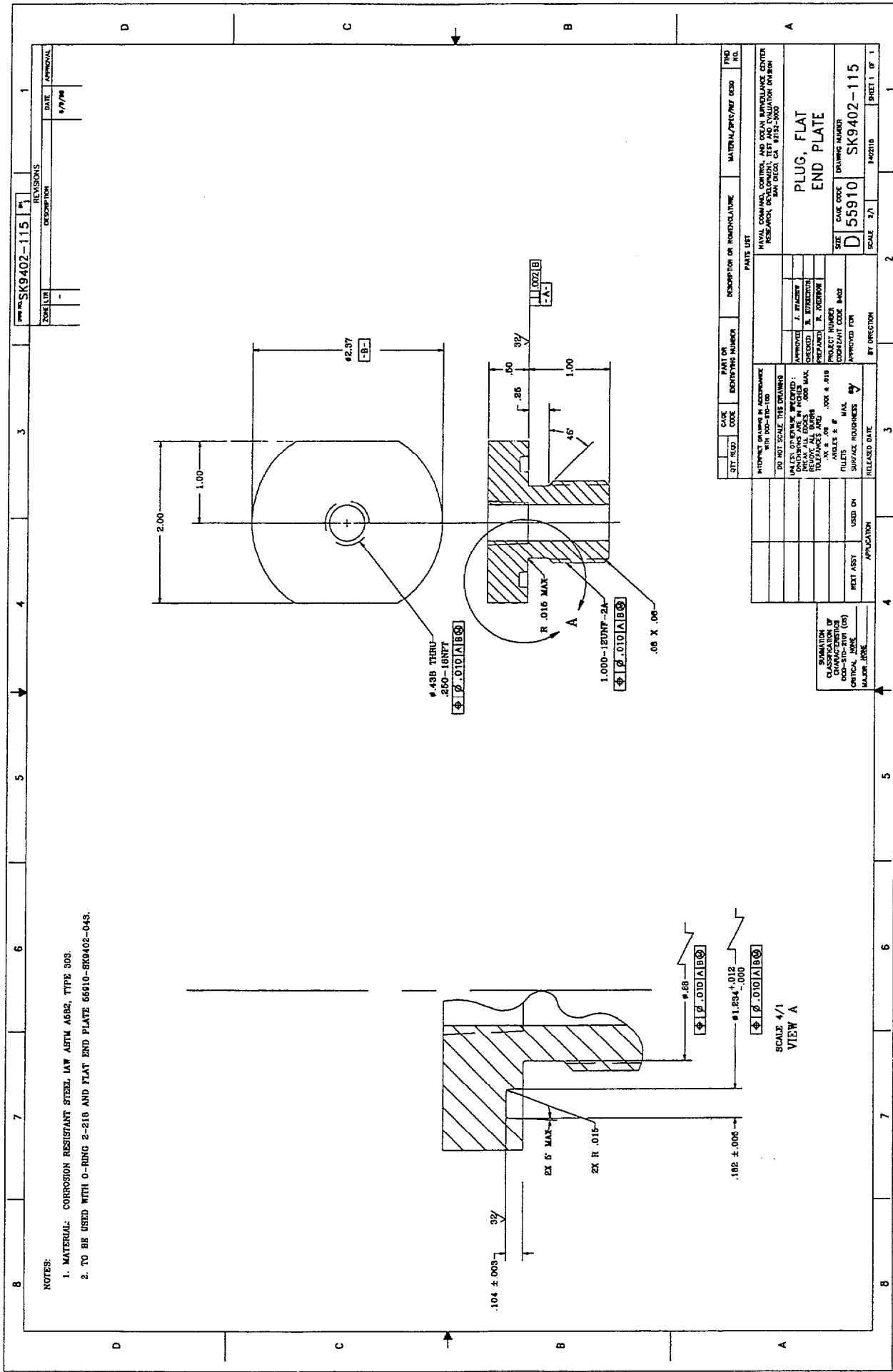


Figure 20. Flat end plate plug.



Figure 21. Bearing surface cracks at the top end of the Test Configuration B cylinder.

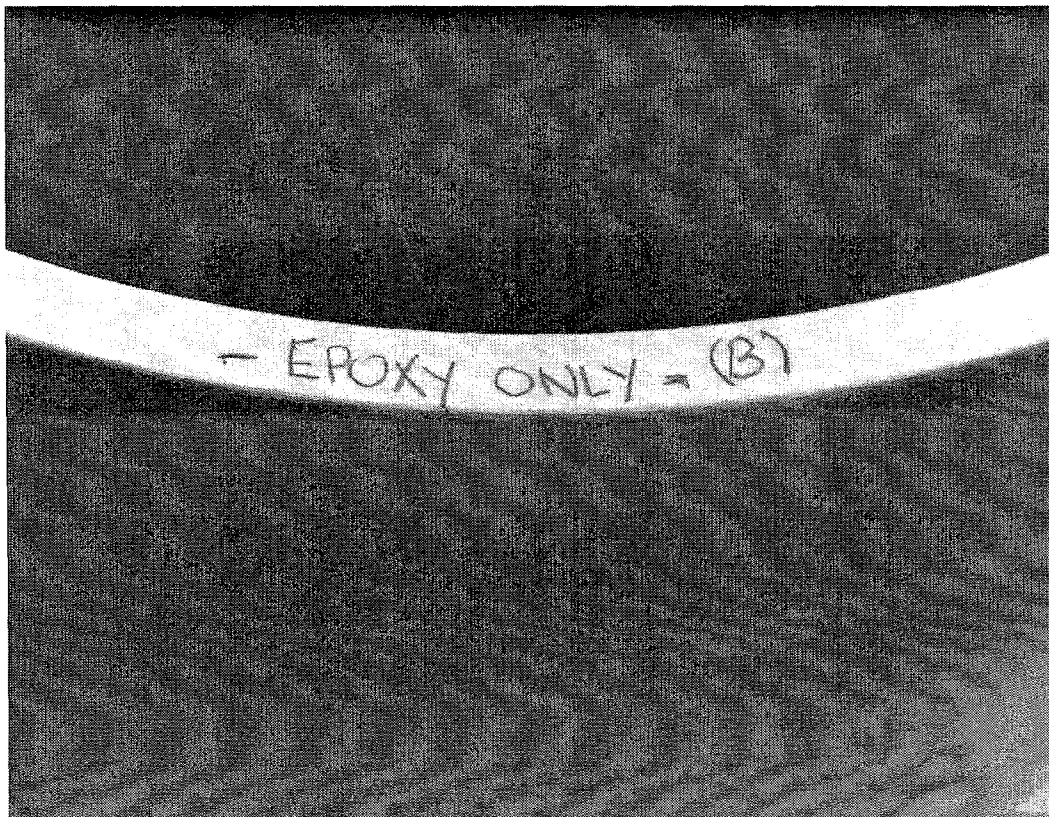


Figure 22. Crack-free bearing surface at the bottom end of the Test Configuration B cylinder.

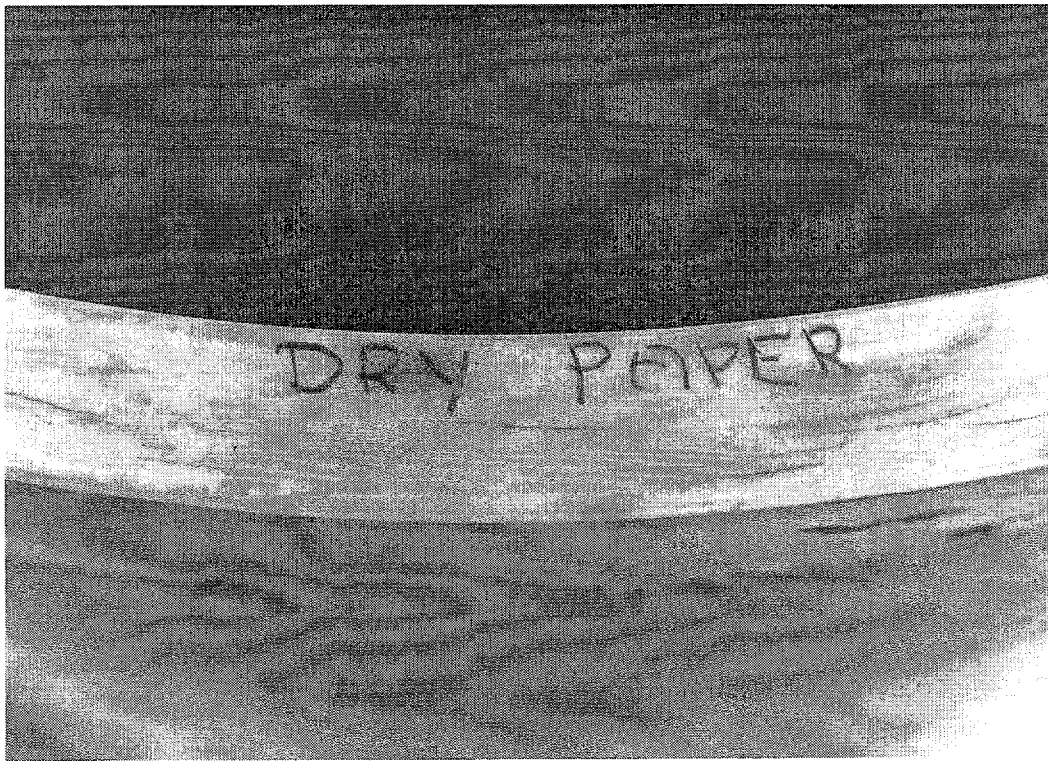


Figure 23. Bearing surface cracks at the top end of the Test Configuration C cylinder.

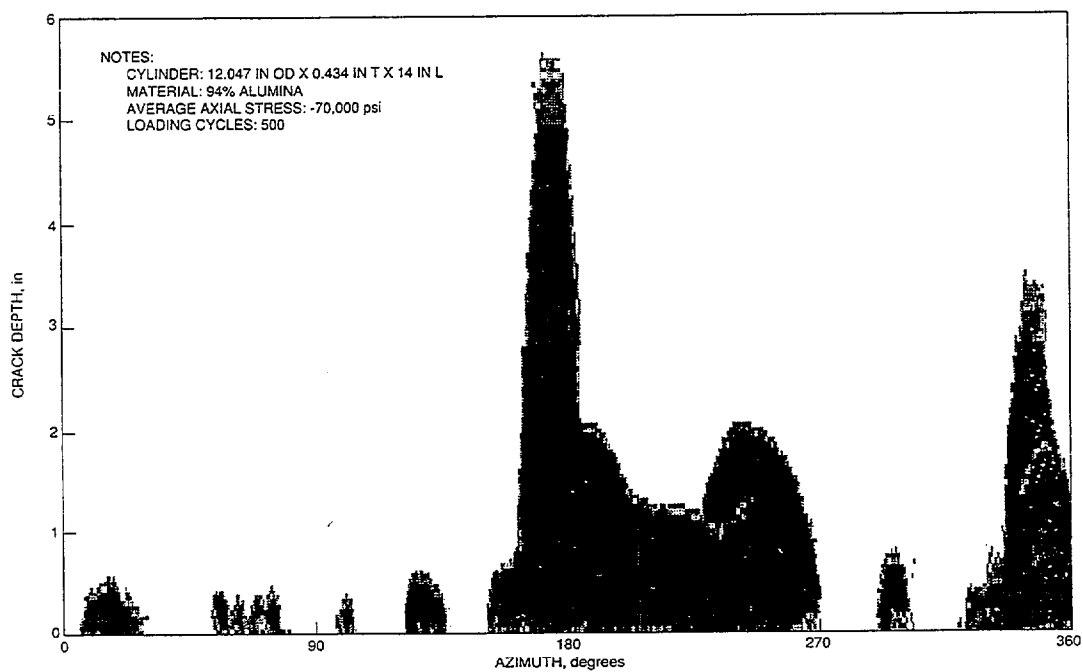


Figure 24. Internal cracks detected ultrasonically at the top end of the Test Configuration A cylinder.

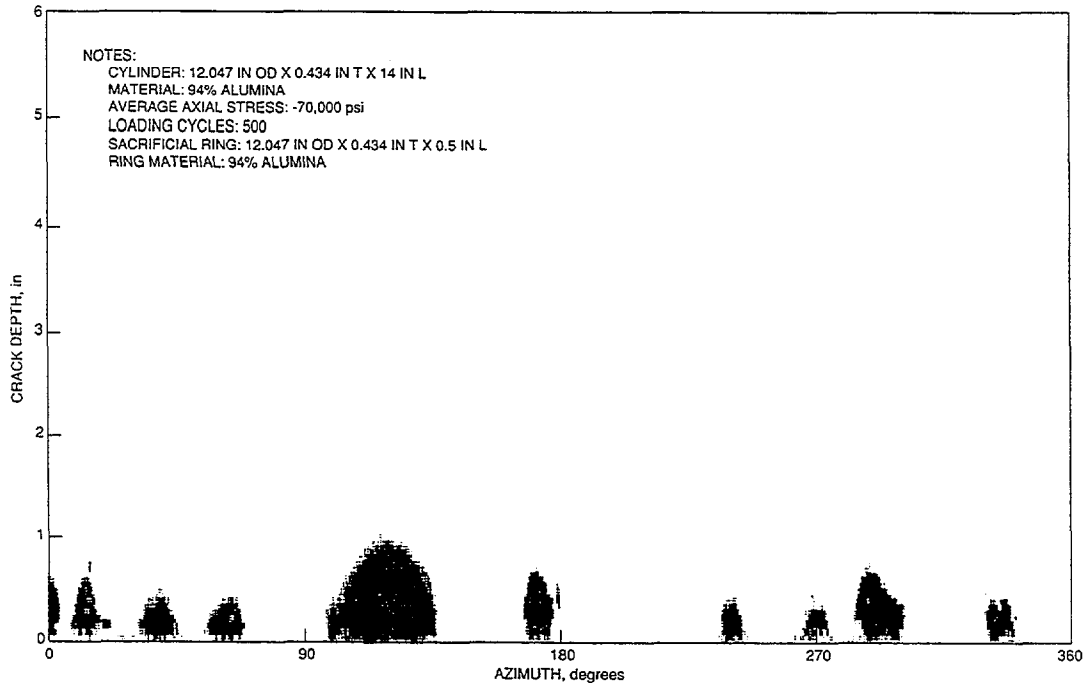


Figure 25. Internal cracks detected ultrasonically at the bottom end of the Test Configuration A cylinder.

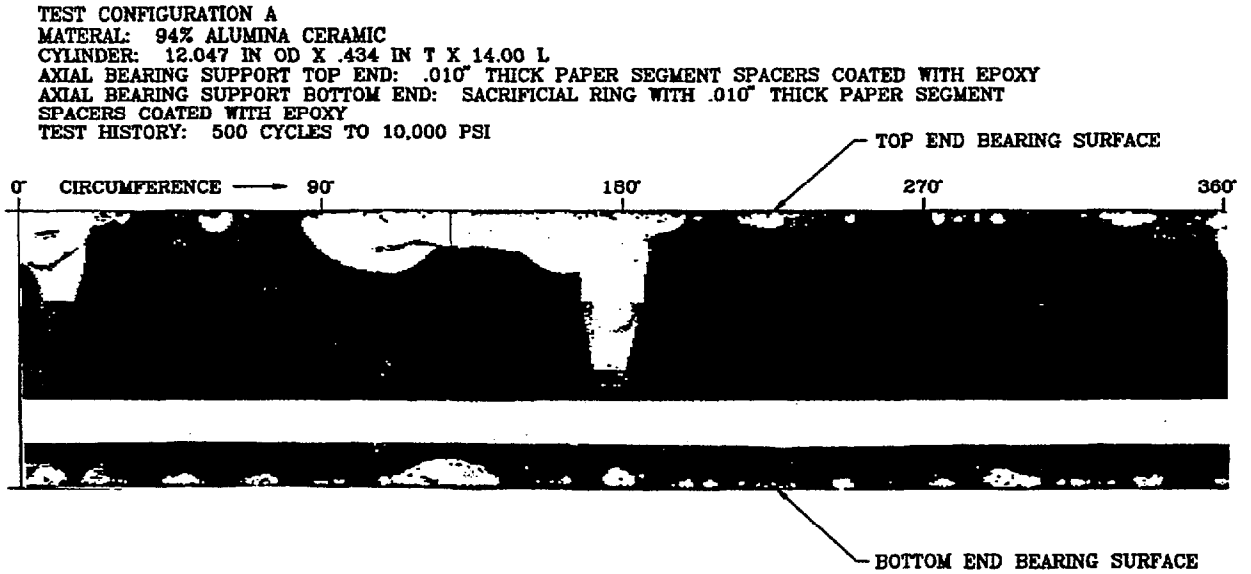


Figure 26. Ultrasonic C-scans of Test Configuration A cylinder ends.

TEST CONFIGURATION B
 MATERIAL: 94% ALUMINA CERAMIC
 CYLINDER: 11.890 IN OD X .355 IN T X 14.00 L
 AXIAL BEARING SUPPORT TOP END: DRY .040" THICK GFR PEEK GASKET
 AXIAL BEARING SUPPORT BOTTOM END: .010" THICK EPOXY LAYER
 TEST HISTORY: 500 CYCLES TO 8,100 PSI

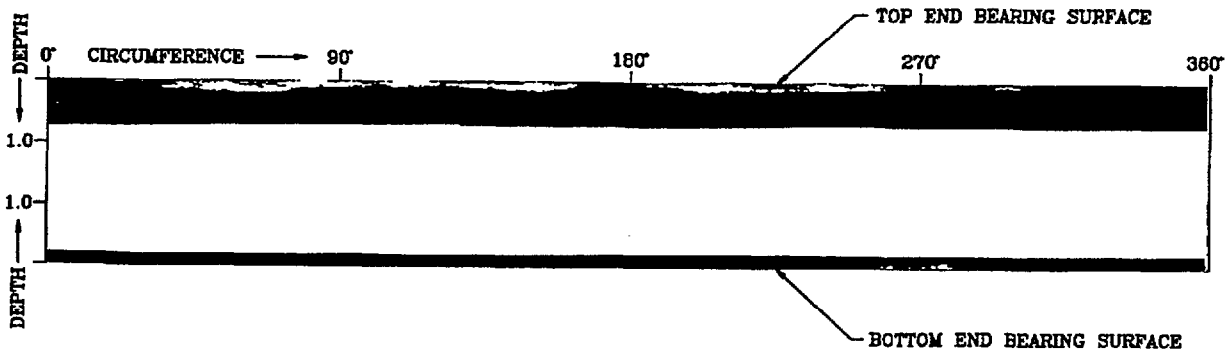


Figure 27. Ultrasonic C-scans of Test Configuration B cylinder ends.

TEST CONFIGURATION C
 MATERIAL: 94% ALUMINA CERAMIC
 CYLINDER: 12.047 IN OD X .434 IN T X 14.00 L
 AXIAL BEARING SUPPORT TOP END: SACRIFICIAL RING WITH .010" THICK DRY PAPER GASKET
 AXIAL BEARING SUPPORT BOTTOM END: SACRIFICIAL RING WITH .010" THICK EPOXY LAYER
 TEST HISTORY: 500 CYCLES TO 10,000 PSI

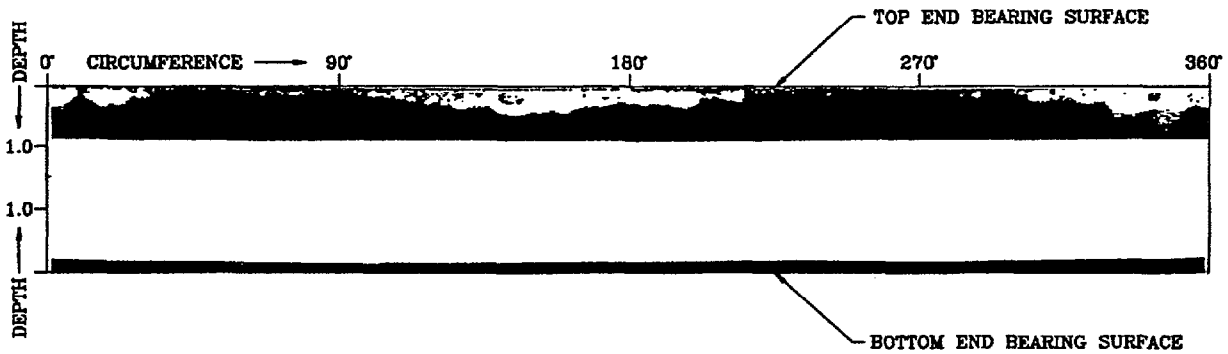


Figure 28. Ultrasonic C-scans of Test Configuration C cylinder ends.

FEATURED RESEARCH

TEST CONFIGURATION D
MATERIAL: 94% ALUMINA CERAMIC
CYLINDER: 11.890 IN OD X .355 IN T X 14.00 L
AXIAL BEARING SUPPORT TOP END: SACRIFICIAL RING WITH .010" THICK PAPER GASKET COATED WITH EPOXY
AXIAL BEARING SUPPORT BOTTOM END: .010" THICK PAPER GASKET COATED WITH EPOXY
TEST HISTORY: 500 CYCLES TO 8,100 PSI

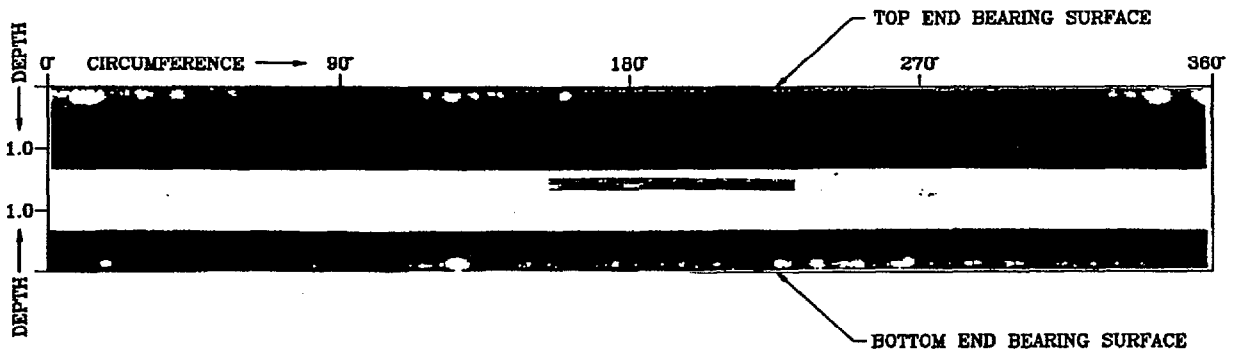


Figure 29. Ultrasonic C-scans of Test Configuration D cylinder ends.

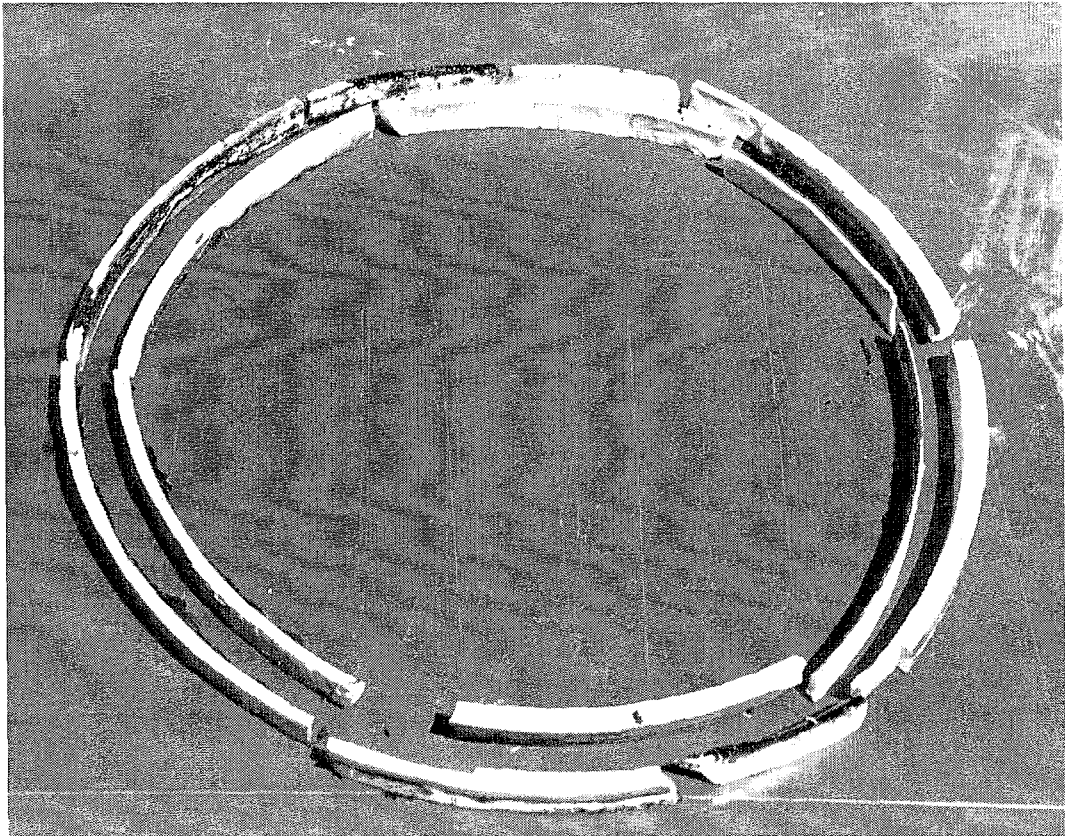


Figure 30. Remains of Test Configuration A sacrificial ceramic ring after pressure testing

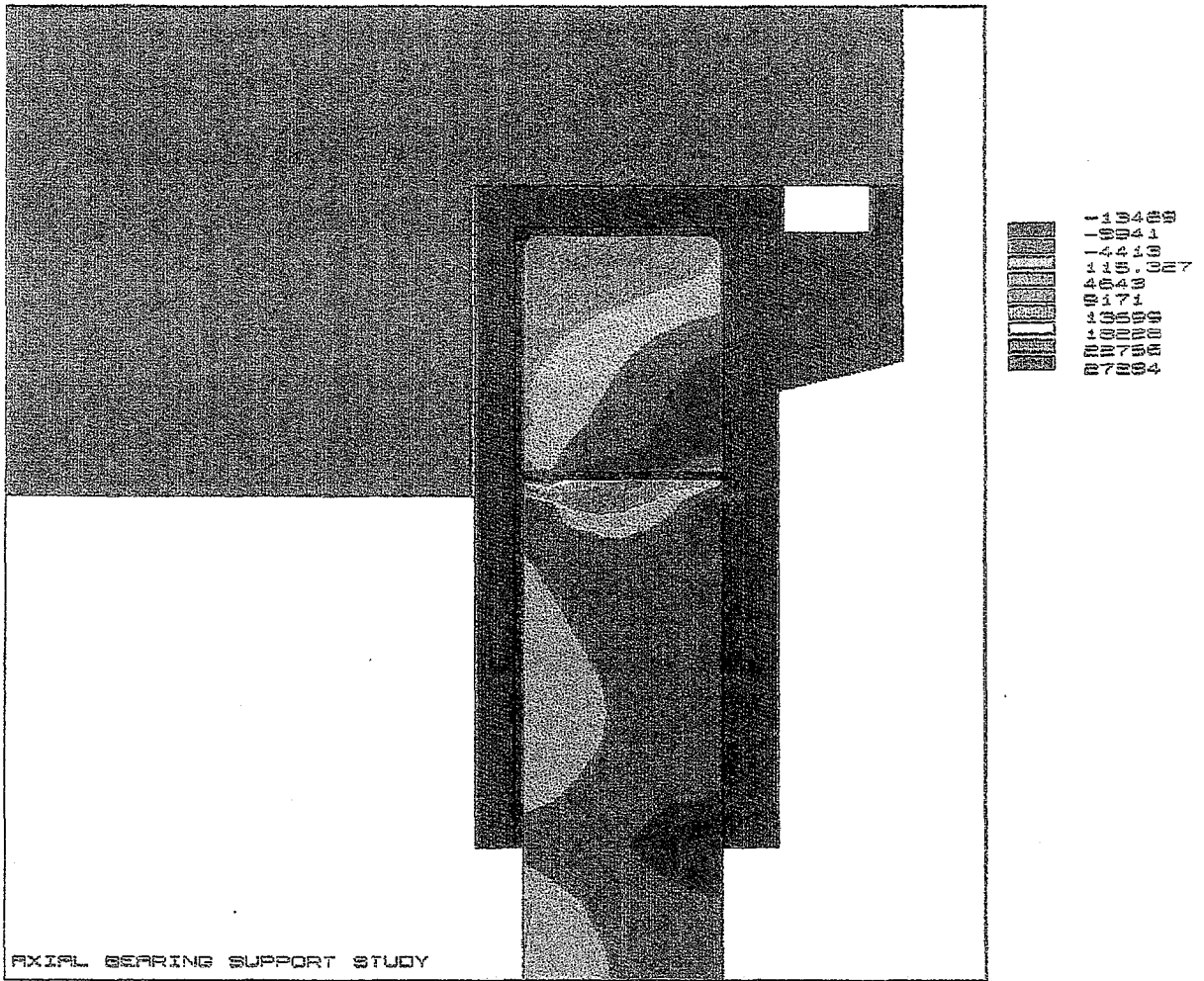


Figure 31. Radial stress-contour plot of ceramic cylinder/ceramic sacrificial ring interface.

Table 1. Material properties of Coors Ceramic Company's alumina-ceramic compositions.

PROPERTIES*	UNITS	TEST	AD-85	AD-90 Nom. 90% Al ₂ O ₃	AD-94 Nom. 94% Al ₂ O ₃	AD-96 Nom. 96% Al ₂ O ₃	AD-995 Nom. 99.5% Al ₂ O ₃
SPECIFIC GRAVITY		ASTM-C20-70	3.41	3.60	3.62	3.72	3.89
HARDNESS ROCKWELL KNOOP	R45N GPa	ASTM E18-67 1000-g load	73 9.8	79 10.8	78 11.1	76 11.1	83 14.7
SURFACE FINISH	AS-FIRED GROUND POUSHED	PROFILOMETER (0.75mm cutoff)	1.8 (83) 1.0 (39) 0.2 (8.0)	1.6 (83) 0.5 (20) 0.1 (3.9)	1.6 (63) 1.3 (51) 0.3 (12)	1.6 (63) 1.3 (51) 0.3 (12)	0.9 (35) 0.5 (20) 0.1 (3.9)
CRYSTAL SIZE	RANGE AVERAGE	MICROMETRES (MICROINCHES)	2-12 (78-473) 6 (236)	2-10 (79-394) 4 (158)	2-25 (79-985) 12 (473)	2-20 (79-788) 11 (433)	5-50 (197-1970) 16 (670)
WATER ABSORP.		ASTM C373-72	NONE	NONE	NONE	NONE	NONE
GAS PERM.**			NONE	NONE	NONE	NONE	NONE
COLOR			WHITE	WHITE	WHITE	WHITE	IVORY
COMPRESSIVE STRENGTH	25°C 1000°C	MPa (kpsi) ASTM C773-74	1930 (280) — (—)	2482 (360) 517 (75)	2103 (305) 345 (50)	2068 (300) — (—)	2620 (380) — (—)
FLEXURAL STRENGTH	TYP., 25°C MIN., 25°C*** TYP., 1000°C MIN., 1000°C***	MPa (kpsi) ASTM F417-75T	296 (43) 289 (39) 172 (25) 138 (20)	338 (49) 303 (44) — (—) — (—)	352 (51) 317 (46) 138 (20) 117 (17)	358 (52) 324 (47) 172 (25) 138 (20)	379 (55) — (—) — (—) — (—)
TENSILE STRENGTH	25°C 1000°C	MPa (kpsi) ACMA TEST -4	155 (22) — (—)	221 (32) 103 (15)	193 (28) 103 (15)	193 (28) 96 (14)	262 (38) — (—)
MOD. OF ELAST. SHEAR MODULUS BULK MODULUS TRANS. SONIC VEL. POISSON'S RATIO	GPa (10 ⁶ psi) GPa (10 ⁶ psi) GPa (10 ⁶ psi) m/sec (ft/sec)	ASTM C623-71	221 (32) 96 (14) 138 (20) 8.2 (27) × 10 ³ 0.22	276 (40) 117 (17) 158 (23) 8.8 (29) × 10 ³ 0.22	283 (41) 117 (17) 165 (24) 8.9 (29) × 10 ³ 0.21	303 (44) 124 (18) 172 (25) 9.1 (30) × 10 ³ 0.21	372 (54) 152 (22) 228 (33) 9.8 (32) × 10 ³ 0.22
MAX-USE TEMP. (No-load conds.)	°C (°F)		1400 (2550)	1500 (2730)	1700 (3100)	1700 (3100)	1750 (3180)
COEFFICIENT OF LINEAR THERMAL EXPANSION	200-25°C 25-200°C 25-500°C 25-800°C 25-1000°C 25-1200°C	10-5/°C (10-9°/F) ASTM C372-56	3.4 (1.9) 5.3 (3.0) 6.2 (3.5) 6.9 (3.9) 7.2 (4.0) 7.5 (4.2)	3.4 (1.9) 6.1 (3.4) 7.0 (3.9) 7.7 (4.3) 8.1 (4.5) 8.4 (4.7)	3.4 (1.9) 6.3 (3.5) 7.1 (4.0) 7.6 (4.3) 7.9 (4.4) 8.1 (4.5)	3.4 (1.9) 6.0 (3.4) 7.4 (4.1) 8.0 (4.5) 8.2 (4.6) 8.4 (4.7)	3.4 (1.9) 7.1 (4.0) 7.6 (4.3) 8.0 (4.5) 8.3 (4.6) —
THERMAL CONDUCTIVITY	20°C 100°C 400°C 800°C	W/m-K (g-cal/(sec)(cm ²) (°C/cm)) ASTM C408-58	14.6 (0.035) 12.1 (0.029) 6.7 (0.016) 4.2 (0.010)	16.7 (0.040) 13.4 (0.032) 7.9 (0.017) 5.0 (0.010)	18.0 (0.043) 14.2 (0.035) 7.9 (0.017) 5.0 (0.010)	24.7 (0.059) 18.8 (0.045) 10.0 (0.024) 5.4 (0.013)	35.6 (0.085) 25.9 (0.062) 12.1 (0.028) 6.3 (0.015)
SPECIFIC HEAT	100°C	J/kg-K (cal/g/°C) ASTM C351-61	920 (0.22)	920 (0.22)	880 (0.21)	880 (0.21)	880 (0.21)

Table 2. Material properties of the cured epoxy bonds between titanium joint rings and alumina-ceramic hulls.

Castings	Parts by weight
Araldite GY 6010	100
Hardener XU HY 283 (Supplied by Ciba-Geigy)	70
Preparation	
Resin and hardener were degassed separately and mixed thoroughly by hand. The mixture was then degassed to eliminate air bubbles.	
Cure schedule (18-in casting)	7 days at 23°C
Tensile Properties	
(at 23°C unless otherwise noted)	
Tensile strength (psi)	4,700
Yield elongation (%)	3.6
Break elongation (%)	26.1
Tensile Modulus (psi)	
at 23°C	272,500
at 0°C	300,300
at -20°C	314,100
at -40°C	323,400
at -100°C	355,700
Compressive Properties	
Compressive strength (psi)	13,400
Compressive modulus (psi)	328,000
Yield compression (%)	5.3
Ultimate compression (psi)	34,200
Ultimate compression (%)	53.7
Flexural Properties	
Flexural strength (psi)	7,100
Flexural modulus (psi)	154,000
Lap shear* (psi)	3,700
HDT (°C)	37

* Alclad 2024 T-3 Aluminum Alloy 1/2-in x 1-in lap joint in shear at room temperature.

Table 3. Die-penetrant inspection findings of axial bearing surfaces.

DYE PENETRANT INSPECTION FINDINGS OF AXIAL BEARING SURFACES			
TEST CONFIG.	CYLINDER END	AXIAL BEARING SURFACE SUPPORTING THE CYLINDER END	DYE PENETRANT INSPECTION OBSERVATIONS
A	TOP	.010" THICK PAPER SEGMENT SPACERS COATED WITH EPOXY	SEVERAL LONG CIRCUMFERENTIAL CRACKS AT MID PLANE OF BEARING SURFACE
A	BOTTOM	SACRIFICIAL RING WITH .010" THICK PAPER SEGMENT SPACERS COATED WITH EPOXY	SINGLE MEDIUM LENGTH CIRCUMFERENTIAL CRACK
B	TOP	DRY .040" THICK GFR PEEK GASKET	BRANCHED CIRCUMFERENTIAL CRACKS OVER APPROXIMATELY 270 DEGREES OF BEARING SURFACE
B	BOTTOM	.010" THICK EPOXY LAYER	SEVERAL FAINT SHORT CIRCUMFERENTIAL CRACKS
C	TOP	SACRIFICIAL RING WITH .010" THICK DRY PAPER GASKET	EXTENSIVE DENSE CRACKING OVER MAJORITY OF BEARING SURFACE
C	BOTTOM	SACRIFICIAL RING WITH .010" THICK EPOXY LAYER	NO VISIBLE CRACKS
D	TOP	SACRIFICIAL RING WITH .010" THICK PAPER GASKET COATED WITH EPOXY	SEVERAL SHORT DISCONTINUOUS CIRCUMFERENTIAL CRACKS RANDOMLY SCATTERED OVER BEARING SURFACE
D	BOTTOM	.010" THICK PAPER GASKET COATED WITH EPOXY	SHORT CIRCUMFERENTIAL CRACKS CLUSTERED IN ONE LOCATION

Table 4. Ultrasonic inspection findings of axial bearing surfaces.

ULTRASONIC INSPECTION FINDINGS OF AXIAL BEARING SURFACES				
TEST CONFIG.	CYLINDER END	AXIAL BEARING SURFACE SUPPORTING THE CYLINDER END	ULTRASONIC INSPECTION OBSERVATIONS	MAX CRACK PENETRATION
A	TOP	.010" THICK PAPER SEGMENT SPACERS COATED WITH EPOXY	TWO PRIMARY WELL DEVELOPED CRACKED REGIONS	5.5"
A	BOTTOM	SACRIFICIAL RING WITH .010" THICK PAPER SEGMENT SPACERS COATED WITH EPOXY	NUMEROUS SHORT RANDOMLY LOCATED SHALLOW CRACKS	1.0"
B	TOP	DRY .040" THICK GFR PEEK GASKET	TWO PRIMARY WIDE CRACKS OF UNIFORM SHALLOW DEPTH	0.3"
B	BOTTOM	.010" THICK EPOXY LAYER	ONE SMALL LOCAL AREA WITH SHALLOW CRACKS	0.2"
C	TOP	SACRIFICIAL RING WITH .010" THICK DRY PAPER GASKET	TWO PRIMARY CRACKED REGIONS OF UNIFORM MEDIUM DEPTH	1.7"
C	BOTTOM	SACRIFICIAL RING WITH .010" THICK EPOXY LAYER	NO CRACKS DETECTED	NA
D	TOP	SACRIFICIAL RING WITH .010" THICK PAPER GASKET COATED WITH EPOXY	NUMEROUS SHORT RANDOMLY LOCATED SHALLOW CRACKS	0.5"
D	BOTTOM	.010" THICK PAPER GASKET COATED WITH EPOXY	NUMEROUS SHORT RANDOMLY LOCATED SHALLOW CRACKS	0.5"

THE AUTHORS



RICHARD P. JOHNSON is an Engineer for the Ocean Engineering Division. He has held this position since 1987. Before that, he was a Laboratory Technician for the Ocean Engineering Laboratory, University of California at Santa Barbara from 1985-1986, and Design Engineer in the Energy

Projects Division of SAIC from 1986-1987. His education includes a B.S. in Mechanical Engineering from the University of California at Santa Barbara in 1986, and an M.S. in Structural Engineering from the University of California, San Diego, in 1991. He has published "Stress Analysis Considerations for Deep Submergence Ceramic Pressure Housings," *Intervention '92*, Marine Technology Society. He is a member of the Marine Technology Society.



RAMON R. KURKCHUBASCHE is a Research Engineer for the Ocean Engineering Division and has worked since November 1990 in the field of deep submergence pressure housings fabricated from ceramic materials. His education includes a B.S. in Structural Engineering from the

University of California at San Diego, 1989; and an M.S. in Aeronautical/Astronautical Engineering from Stanford University in 1990. His experience includes conceptual design, procurement, assembly, testing, and documentation of ceramic hous-

ings. Other experience includes buoyancy concepts utilizing ceramic, nondestructive evaluation of ceramic components. He is a member of the Marine Technology Society, and has published "Elastic Stability Considerations for Deep Submergence Ceramic Pressure Housings," *Intervention '92*, Marine Technology Society.



DR. JERRY STACHIW is Staff Scientist for Marine Materials in the Ocean Engineering Division. He received his undergraduate engineering degree from Oklahoma State University in 1955 and graduate degree from Pennsylvania State University in 1961.

Since that time he has devoted his efforts at various U.S. Navy Laboratories to the solution of challenges posed by exploration, exploitation, and surveillance of hydrospace. The primary focus of his work has been the design and fabrication of pressure resistant structural components of diving systems for the whole range of ocean depths. Because of his numerous achievements in the field of ocean engineering, he is considered to be the leading expert in the structural application of plastics and brittle materials to external pressure housings.

Dr. Stachiw is the author of over 100 technical reports, articles, and papers on design and fabrication of pressure resistant viewports of acrylic plastic, glass, germanium, and zinc sulphide, as well as pressure housings made of wood, concrete, glass, acrylic plastic, and ceramics. His book on "Acrylic Plastic Viewports" is the standard reference on that subject.

FEATURED RESEARCH

For the contributions to the Navy's ocean engineering programs, the Navy honored him with the Military Oceanographer Award and the NCCOSC's RDT&E Division honored him with the Lauritsen-Bennett Award. The American Society of Mechanical Engineers recognized his contributions to the engineering profession by election to the grade of Life-Fellow, as well as the presentation of Centennial Medal, Dedicated Service Award and Pressure

Technology Codes Outstanding Performance Certificate.

Dr. Stachiw is past-chairman of ASME Ocean Engineering Division and ASME Committee on Safety Standards for Pressure Vessels for Human Occupancy. He is a member of the Marine Technology Society, New York Academy of Science, Sigma Xi and Phi Kappa Honorary Society.

Authorized for public release; distribution is unlimited.